

REVIEWS OF MODERN PHYSICS

VOLUME 5

JULY, 1933

NUMBER 3

On the Factors Affecting the Reflection Intensities by the Several Methods of X-Ray Analysis of Crystal Structures

F. C. BLAKE, *Mendenhall Laboratory of Physics, Ohio State University*

CONTENTS

I. THEORETICAL CONSIDERATIONS	169
II. INTENSITY FACTORS FOR THE POWDER METHOD	170
1. Polarization factor	170
2. Lorentz factor	171
3. Temperature factor	175
4. Absorption factor	178
5. Structure factor	185
6. Atomic form factor	186
7. Form or multiplicity factor	190
III. COMPARISON WITH EXPERIMENT	192
IV. CORRECT PROCEDURE IN INTERPRETING THE DENSITOMETER WORK	192
V. TEST OF INTENSITY FORMULA	194
VI. ANOMALOUS DISPERSION AS REVEALED IN THE DETERMINATION OF THE ATOMIC SCATTERING POWER	196
VII. CONCLUSION	200
VIII. ACKNOWLEDGMENTS	201
BIBLIOGRAPHY	201

IT is well known that there are four methods of x-ray analysis of crystal structures: (1) the spot method of von Laue,¹ (2) the powder method of Debye-Scherrer² and Hull,³ (3) the ionization spectrometer method of the Braggs,⁴ (4) the rotating (oscillating) crystal method of Seemann,⁵ Schiebold⁶ and Polanyi.⁷

I. THEORETICAL CONSIDERATIONS

The first adequate theoretical attempt to account for the intensity of x-ray reflection was given by Darwin⁸ in a series of three papers. In his second paper Darwin allows for the mutual reactions of the scattering atoms. In his third paper he handles the matter of extinction, experi-

mentally encountered by Bragg, James and Bosanquet.⁹ Darwin distinguishes between primary and secondary extinction, primary extinction "consisting in the reduction of the beam reflected from a perfect crystal owing to the defect in the radiation reaching its lower layers," and secondary extinction "consisting in the reduction in intensity of the transmitted beam on emerging from the lower side of a small crystal in which some reflection has taken place," to quote Darwin's original wording in each case. He states that the methods used by Bragg, James and Bosanquet removed the secondary extinction but didn't touch the primary extinction. However, Havighurst¹⁰ found it necessary

to apply their correction for secondary extinction to their results for rocksalt to get agreement with his own best (Sample 3) results. He states that when the crystal particles become as small as 10^{-2} to 10^{-3} cm in size, secondary extinction becomes negligible but that primary extinction remains appreciable until the size of the perfect crystal blocks becomes less than 5×10^{-6} cm.

This figure is derived from the correction factor worked out by Darwin for primary extinction, *viz.*,

$$Q' = Q \frac{\tanh [(2Qd^2 \cot \theta)/\lambda]^{\frac{1}{2}}}{[(2Qd^2 \cot \theta)/\lambda]^{\frac{1}{2}}}, \quad (1)$$

the coefficient of Q on the right-hand side being almost equal to unity only for crystals smaller than 5×10^{-6} cm when rhodium rays are used, d being the crystal thickness.

Now there has never been any satisfactory testing of this or other extinction formulas although it is known that the errors due to ignoring the effects of extinction are large. It has already been mentioned that Bragg, James and Bosanquet corrected their results on rocksalt for secondary extinction but Havighurst found that the correction for secondary extinction applied by James and Randall^{10a} did not bring their results for fluorite into agreement with his own. Havighurst showed moreover that both primary and secondary extinction are eliminated for very finely powdered crystals and it is this fact that up to date has rendered the powder method alone the only true precision method. For this reason the intensity formulas for the powder method are discussed in this survey. Much further investigation is sorely needed, especially for crystals containing atoms of large atomic number before one is safe in saying that there is no error due to primary extinction for very finely divided crystals.

II. INTENSITY FORMULA FOR THE POWDER METHOD

1. Polarization factor

The question of the polarization of the x-rays emitted by the anticathode of an x-ray tube has never been adequately investigated as a function of the hardness of the rays emitted, as a function of the direction of the rays coming from the anti-

cathode, though a good deal of work has been done. However, the work of Bearden^{10b} and of Wollan^{10c} seems conclusively to prove that the characteristic rays, at least, are unpolarized. In discussing the scattering of x-rays by matter it is customary to assume the primary rays as unpolarized and various experimenters¹¹ have found good agreement between their results and the classical theory of scattering, first worked out by Sir J. J. Thomson,¹² whereby the factor $\frac{1}{2}(1 + \cos^2 2\theta)$ has come to be known as the Thomson polarization factor. This factor is readily determined in the following way. If E is the electric force in the primary x-ray making an angle θ with the face of a crystal, the electric force making an angle ϕ with the positive x-axis, the energy in the secondary beam would be proportional to

$$E^2 \sin^2 \phi + E^2 \cos^2 \phi \cos^2 2\theta = E^2(1 - \cos^2 \phi \sin^2 2\theta)$$

and the total energy of the secondary beam is proportional to $\int_0^{2\pi} (1 - \cos^2 \phi \sin^2 2\theta) d\phi$ that is proportional to $\frac{1}{2}(1 + \cos^2 2\theta)$. Putting this in another way one can say that an unpolarized ray can be said to have two equal unit electric vectors each of amplitude $\frac{1}{2}(2)^{\frac{1}{2}}$. (Fig. 1.)

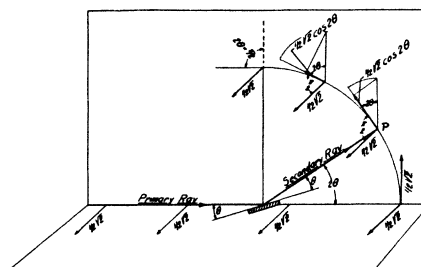


FIG. 1.

At the point P the horizontal vector is acting with full effect but the vertical vector V has only the component $\frac{1}{2}(2)^{\frac{1}{2}} \cdot \cos 2\theta$ effective, for it is known that an electric doublet radiates zero energy in a direction parallel to the axis of the doublet. The intensity at P which is proportional to the square of the amplitude thus has the value $\frac{1}{2}(1 + \cos^2 2\theta)$. There is no distinction between the various methods of analysis as to this factor; hence it is common to all methods.

2. Lorentz factor

A second factor upon which the reflection intensity depends is the so-called Lorentz factor. This arises from the fact that in the various methods of crystal analysis (except those where the primary beam consists of a strictly monochromatic beam such as one gets after reflection from a single crystal such as calcite) the primary beam is not strictly monochromatic, nor is the beam a parallel one but generally divergent.

Suppose a primary beam of x-rays makes the angles $\alpha_0, \theta_0, \gamma_0$ with the three axes of a crystal, such that one can say that the three edges a, b, c of the unit lattice of the crystal constitute a volume grating with the spacings a, b, c in the three directions of the axes. Then if one considers the secondary beam as having the direction α, β, γ with the crystal axes it is well known that the v. Laue relations hold

$$\left. \begin{aligned} a(\cos \alpha - \cos \alpha_0) &= h\lambda \\ b(\cos \beta - \cos \beta_0) &= k\lambda \\ c(\cos \gamma - \cos \gamma_0) &= l\lambda \end{aligned} \right\}, \quad (2)$$

where h, k, l are whole numbers, the so-called Miller indices.

Now in the differential equation for spherical waves, viz.,

$$\frac{\partial^2 u}{\partial t^2} = v^2 \left(\frac{\partial^2 u}{\partial x^2} + \frac{\partial^2 u}{\partial y^2} + \frac{\partial^2 u}{\partial z^2} \right), \quad (3)$$

the solution is

$$u = (A/r) \cos(\omega' r - \omega t) = (A/r) \cos(r/\lambda - t/\tau),$$

where

$$r^2 = x^2 + y^2 + z^2 \quad \text{and} \quad v^2 = \omega^2/\omega'^2 = \lambda^2/\tau^2 = \nu^2/\nu'^2$$

with

$$\nu = \omega'/2\pi = 1/\lambda \quad \text{and} \quad \nu' = \omega/2\pi = 1/\tau.$$

The various points of the volume grating are given by their position vectors

$$r_{\lambda\mu\nu} = \lambda\mathbf{a} + \mu\mathbf{b} + \nu\mathbf{c} \quad (\lambda, \mu, \nu = 0, 1, \dots, m-1). \quad (4)$$

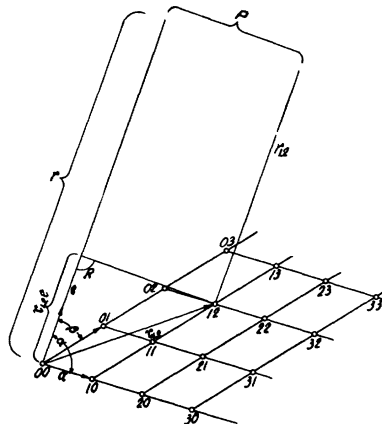


FIG. 2.

For the sake of clearness, thinking in two dimensions only, as drawn in Fig. 2, one sees at once

$$r_{\lambda\mu} = r - (r_{\lambda\mu} \cdot \mathbf{e}) = r - \lambda(\mathbf{a} \cdot \mathbf{e}) - \mu(\mathbf{b} \cdot \mathbf{e}),$$

where \mathbf{e} is a unit vector drawn in the direction of the secondary ray and each parenthesis represents the scalar product of the two vectors within it. But the angle between \mathbf{a} and \mathbf{e} is α , between \mathbf{b} and \mathbf{e} it is β and between \mathbf{c} and \mathbf{e} it is γ . Hence for three dimensions one can write at once

$$\left. \begin{aligned} r_{\lambda\mu\nu} &= r - (r_{\lambda\mu\nu} \cdot \mathbf{e}) \\ &= r - \lambda(\mathbf{a} \cdot \mathbf{e}) - \mu(\mathbf{b} \cdot \mathbf{e}) - \nu(\mathbf{c} \cdot \mathbf{e}) \\ &= r - \lambda a \cos \alpha - \mu b \cos \beta - \nu c \cos \gamma \end{aligned} \right\}. \quad (5)$$

If, now, again for the sake of clearness, one thinks of a linear grating with the grating space a (Fig. 3) one sees from the figure that $r_0 = r, r_1 = r - d, \dots, r_n = r - nd$ where $d = a \cos \alpha$. If now the waves sent out by all the points of the grating have the same amplitude and the same phase then the resultant solution is given by the super-

atoms. It should increase with the thickness of radiated material but within the crystal the rays suffer absorption which is greater the greater the thickness. This so-called absorption factor will be discussed shortly.

Since the differential $dx dy dz$ has no direct physical meaning the $|u|^2$ integral does not represent the integrated intensity. Rather it is the differential of $\alpha\beta\gamma\alpha_0\beta_0\gamma_0\lambda$ connected as above with x, y, z that does that; but because of the interconnection between α, β and γ only five instead of seven quantities are needed. Thus the integrated intensity becomes $I = \int |u|^2 d\alpha d\beta d\alpha_0 d\beta_0 d\lambda$. If, however, we allow only three of the variables to vary at one time we can write

$$I = \int |u|^2 dx dy dz = \int F |u|^2 du dv dw, \quad (11)$$

where F is the functional determinant belonging to the transformation of variables.† By geometrical considerations we proceed to calculate this determinant. Introduce the vector $\mathbf{r} = u\mathbf{a}^* + v\mathbf{b}^* + w\mathbf{c}^*$ where $\mathbf{a}^*, \mathbf{b}^*, \mathbf{c}^*$ are the edges of the reciprocal lattice and related to the edges of the customary space lattice by means of the equation

$$dV = (\mathbf{a}^*[\mathbf{b}^*\mathbf{c}^*]) du dv dw = du dv dw / (\mathbf{a}[\mathbf{bc}]). \quad (12)$$

We can consider this volume element in another way by first considering the vector

$$\mathbf{r} = \nu(\lambda\mathbf{r}) = \nu(\mathbf{e} - \mathbf{e}_0) \quad (\text{Fig. 5}), \quad (13)$$

getting a volume element by variation. Now we can make either ν variable or \mathbf{e} or \mathbf{e}_0 . By varying ν we can obtain the total energy in the element of solid angle $d\Omega$. Varying \mathbf{e}_0 means the primary beam is polychromatic making an element $d\omega$ of a light cone. Now we can keep \mathbf{e}_0 constant and think of the crystal (or the reciprocal grating) as being rotated through the solid angle $d\omega$.

We must now distinguish two cases of practical importance.

First, we can make \mathbf{e} vary through the solid angle $d\Omega$ and we can vary λ by the amount $d\lambda$, ν changing to $\nu' = \nu + d\nu$. Representing $d\Omega$ in Fig. 5 between the unit vectors \mathbf{e}_1 and \mathbf{e}_2 we keep λ constant and call the vector E_0E_1 , closing the triangle with sides \mathbf{e}_0 and \mathbf{e}_1 , $\lambda\mathbf{r}$. If we multiply

† See M. Laue, *Enz. d. Math. Wiss.* Vol. 5, *Wellenoptik*.

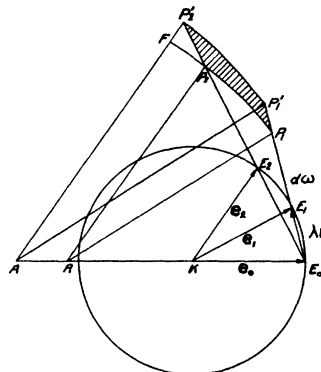


FIG. 5.

this vector by $\nu = AE_0 = AP_1 = AP_2$ we get the vector $E_0P = \mathbf{r}$ whose end points lie on the cone of radius ν . The surface area over which the point P can play is accordingly $\nu^2 d\Omega$. If now we vary λ by the amount $d\lambda$ then the region P_1P_2 goes over into $P_1'P_2'$ lying on a cone of radius ν' . Thus the point P describes the element of volume dV given by the product of the surface element $\nu^2 d\Omega$ and the height FP_2' . Now in the right-angled triangle FP_2P_2' , $P_2P_2' = E_0E_2 d\nu = 2 \sin \theta d\nu$ since the angle $FP_2P_2' = \theta$. Then $FP_2' = 2 \sin^2 \theta d\nu$ giving $dV = 2\nu^2 \sin^2 \theta d\nu d\Omega$. But from Eq. (13) we get $r = 2\nu \sin \theta$ since $\mathbf{e} - \mathbf{e}_0 = 2 \sin \theta$ giving

$$dV = \frac{1}{2} r^2 d\nu d\Omega. \quad (14)$$

By comparing (12) and (14) we get

$$d\nu d\Omega = 2 du dv dw / r^2 (\mathbf{a}[\mathbf{bc}]). \quad (14a)$$

Calling the intensity I integrated over $d\nu$ and $d\Omega$ we get from (11)

$$I_L = [2 / (\mathbf{a}[\mathbf{bc}])] \int (|u|^2 / r^2) du dv dw. \quad (15)$$

Here the subscript L refers to the Laue method using white radiation. This integral can be simplified by replacing r^2 by $(4 \sin^2 \theta) / \lambda^2$ and remembering (10). Thus we get

$$I_L = \frac{A^2 m m' m''}{2 (\mathbf{a}[\mathbf{bc}]) \sin^2 \theta} = \frac{2 A^2 m m' m'' d^2}{n^2 (\mathbf{a}[\mathbf{bc}])} \quad (16)$$

because of the Bragg relation

$$n\lambda = 2d \sin \theta. \quad (17)$$

The factor $\lambda^2/2 \sin^2 \theta$ can be called the white or polychromatic Lorentz factor. Thus the intensity in the Laue spot method, using white radiation, varies inversely as the square of the order of interference. It is greater, too, the smaller the indices of the plane considered since

$$d = 1/|\mathbf{h}| \quad (18)$$

where

$$|\mathbf{h}| = |h\mathbf{a}^* + k\mathbf{b}^* + l\mathbf{c}^*|. \quad (19)$$

This polychromatic Lorentz factor was first given by Professor Lorentz to his classes, it appearing in the literature first as an addendum to the paper of Professor Debye on his temperature factor for intensities.*

Second, we can vary \mathbf{e} by the angle $2d\theta$ and the position of the crystal by the solid angle $d\omega$. Thus in Fig. 6 the end point of the vector \mathbf{r}

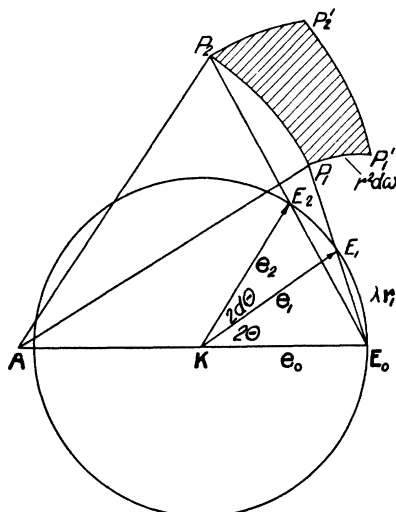


FIG. 6.

describes the line element P_1P_2 . If the crystal is rotated through the solid angle $d\omega$ then P_1P_2 describes in the space of the reciprocal grating a volume element dV given by the product of the surface $r^2 d\omega$ by the corresponding height $E_0P_2 - E_0P_1 = dr$. Now by differentiating the equation $\lambda r = 2 \sin \theta$ we get $\lambda dr = 2 \cos \theta d\theta$ whence

$$dV = r^2 dr d\omega = (2r^2 \cos \theta d\theta d\omega) / \lambda. \quad (20)$$

* Debye, Ann. d. Physik 43, 93 (1913-14).

By comparing (12) with (20) we get

$$2d\theta d\omega = \frac{\lambda d\omega dr d\omega}{r^2 \cos \theta (a[bc])} = \frac{\lambda}{2 \cos \theta} d\omega dr d\omega,$$

because of (14a).

If we call the corresponding intensity factor I_D (D = Debye) then we have

$$I_D = I_L \frac{\lambda}{2 \cos \theta} = \frac{A^2 m m' m'' \lambda^3}{4(a[bc]) \sin^2 \theta \cos \theta}. \quad (21)$$

This factor is known as the monochromatic Lorentz factor and was first given by Debye and Scherrer,* and it is stated that the proof of the formula would be given later. This monochromatic Lorentz factor obviously applies to the powder method where the sample is rotated, filtered rays being used. For a given substance since the wave-length is held constant one can say that the Lorentz factor for the powder method varies inversely as $2 \sin^2 \theta \cos \theta = \sin 2\theta \sin \theta$, the usual expression found in the literature. The discussion of these two important cases for the Lorentz factor is taken more or less bodily from Schleede and Schneider's *Röntgenspektroskopie und Kristallstrukturanalyse*.† This two volume work is one of the best published on the whole field of crystal structure work by means of x-rays.

Darwin in his third paper‡ shows for a single crystal that the Lorentz factor is proportional to $\csc 2\theta$ as does Professor Compton (*X-Rays and Electrons*, p. 125). For a thick plate of powdered crystals Compton shows (p. 130) it proportional to $\csc 2\theta \csc \theta$, the expression used by Havighurst.¶ This is in agreement with (21). It is obvious that this same expression holds for cylindrical rods of powdered crystals, provided there is no "preferred orientation" of the crystals such as always comes from forcing the powdered crystals through a die.

It is important for the reader to get the significance of the distinctions developed in the two cases of the Lorentz factor. In the first case the frequency or wave-length was varied, while in the second it was not. Again, in the first method

* Debye and Scherrer, Phys. Zeits. 19, 481 (1918).

† Vol. II, 240-244 (1929), Walter de Gruyter & Co., Berlin and Leipzig.

‡ Darwin, Phil. Mag. 43, 808 (1922).

¶ Havighurst, Phys. Rev. 28, 873 (1926).

the change in direction is through a solid angle and the wave-length variable, thus this case applies directly to the Laue method for single crystals. On the other hand, in the second case the direction changes through a plane angle (oscillation or rotation of the powder sample) and the crystal through a solid angle (random orientation of all the very small crystals making up the powder). Hence this second case should cover the practice of modern powder methods, whether briquets or rods of finely powdered crystals are used.

3. Temperature factor

A third factor upon which the powder and other methods depend is the so-called Debye temperature factor. It is obvious from general considerations of molecular and atomic agitation due to heat that the atoms in a crystal lattice vibrate about their equilibrium positions. As the vibrations increase in intensity with temperature rise the chance for x-ray interferences is proportionately lessened, the clearness of these interferences for all methods of analysis decreases, becoming zero when a sufficiently high temperature is reached.

The influence of temperature upon x-ray reflection has been handled theoretically by Debye,¹³ v. Laue,¹⁴ Darwin,¹⁵ Schrödinger,¹⁶ Faxen,¹⁷ Brillouin¹⁸ and Waller.¹⁹ In the literature comparison between theory and experiment has been largely made with the theory as formulated by Debye and some of the experiments seem to agree best with the modification he made to include the case of the zero-point energy being other than zero. Other experiments seem to support the theory where the zero point energy is taken to be zero.

In his earlier papers Debye supposed each atom to be bound by a quasi-elastic force to a position of equilibrium at one of the lattice-points of the crystal. Heat motion displaces the atom from its equilibrium position. Were all the displacements at any time known the effect on the intensity of the beam of x-rays diffracted in any direction could be calculated. By carrying through the calculation for a given configuration, multiplying the intensity factor so obtained by the probability of occurrence of the configuration, and then summing for all possible configurations,

Debye obtained a value for the mean intensity in a given direction. Maxwell's distribution law was applied in getting the probability of a given set of displacements. Thus he showed the intensity of the beam in any direction consisted of two parts, the incoherent (or Compton) scattering and the coherent part or interference maxima. Increased temperature tends to increase the scattered radiation and to decrease the intensity of the interference maxima. In his earlier papers Debye showed that the intensity of the scattered radiation contained a temperature factor $1 - e^{(-16\pi^2 k T \sin^2 \theta) / \lambda^2}$, while that of the interference maxima contained the temperature factor $e^{(-16\pi^2 k T \sin^2 \theta) / f}$ where T is the absolute temperature, k the gas constant, f the quasi-elastic force per unit displacement of the atom, and 2θ the angle between the incident and diffracted beams.

But the use of the Maxwell-Boltzmann distribution law is equivalent to assuming that the displacements of the atoms are all independent, which is not true. For the atoms are bound one to another rather than to a fixed position of equilibrium and the displacement of one disturbs those of neighboring atoms. Born and Karman²⁰ showed in 1913 that the heat motions of the atoms in a crystal may be considered as a series of "elastic waves." So Debye in his last paper recalculated the influence of heat motion on the interference maxima on the basis of quantum theory.

Debye shows, if zero point energy be assumed, that the influence of temperature is to introduce the factor e^{-2M} † into the intensity formula for x-ray interferences, where M is given by the equation

$$M = \frac{6h^2 \sin^2 \theta}{mk\Theta \lambda^2} \left\{ \frac{\phi(x)}{x} + \frac{1}{4} \right\}, \quad (22)$$

where m is the mass of the atom, h is Planck's constant, k the gas constant and Θ the so-called characteristic temperature, equal to $h\nu_m/k$ where ν_m is the maximum frequency of the elastic spectrum, λ being the wave-length and θ the glancing angle. In (22)

$$\phi(x)/x = (1/x^2) \int_0^x \xi d\xi / (e^\xi - 1)$$

and x is the ratio of the characteristic temperature of the crystal to its actual temperature,

† Corrected by Waller, Zeits. f. Physik 17, 406 (1923).

expressed in degrees absolute. Debye shows that

$$\phi(x) = 1 - \frac{x}{4} + \frac{x^2}{36} - \frac{x^4}{3600} + \frac{x^6}{211680} - \frac{x^8}{10886400} + \dots$$

holds for small values of x and

$$\phi(x) = \frac{\pi^2}{6} \frac{1}{x} - e^{-x} \left(1 + \frac{1}{x} \right) - e^{-2x} \left(\frac{1}{2} + \frac{1}{4x} \right) - e^{-3x} \left(\frac{1}{3} + \frac{1}{9x} \right) - \dots$$

holds for large values of x . He gives the following table, Table I, connecting x and $\phi(x)$.

TABLE I.

x	$\phi(x)$	x	$\phi(x)$	x	$\phi(x)$	x	$\phi(x)$
0	1	1.2	0.740	3	0.483	9	0.183
0.2	0.951	1.4	0.704	4	0.388	10	0.164
0.4	0.904	1.6	0.669	5	0.321	12	0.137
0.6	0.860	1.8	0.637	6	0.271	14	0.114
0.8	0.818	2.0	0.607	7	0.234	16	0.103
1.0	0.778	2.5	0.540	8	0.205	20	0.0822

Now from the Bragg relation, $n\lambda = 2d \sin \theta$, one sees that in the expression for M one can substitute $n/2d$ and since n is fixed for a given face and d is fixed at a definite temperature it is obvious that the Debye temperature factor is independent of λ , the wave-length of x-rays used. This is to be expected, of course, from the fundamental principles of heat agitation.

Debye has plotted both $\phi(x)/x$ and $(\phi(x)/x) + \frac{1}{4}$ against $1/x = T/\Theta$. The results are shown in

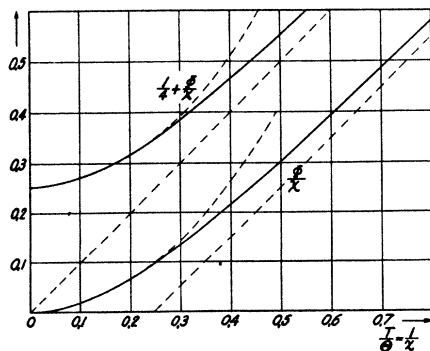


FIG. 7.

Fig. 7. The two curves shown lie between the two approximations

$$\phi/x = (\pi^2/6)T^2/\Theta^2 \text{ and } \phi/x = T/\Theta - \frac{1}{4}$$

for the case of no zero point energy, and between

$$\phi/x + \frac{1}{4} = (\pi^2/6)T^2/\Theta^2 + \frac{1}{4} \text{ and } \phi/x = T/\Theta$$

for the case of zero-point energy. Debye points out that the approximations hold for low temperatures up to $T/\Theta = \frac{1}{4}$ while for high temperatures the corresponding approximation holds from $T/\Theta = 1.6$ on with an error not greater than one percent.

Waller¹⁹ has followed Born²¹ in his theory of the normal coordinates of a crystal lattice. He has developed a method different from that of Debye for connecting the amplitudes of the atomic vibrations with the normal vibrations of the crystal. Waller objects²² to Born's treatment for determining the normal coordinates of the lattice on the basis that they are not independent and develops a method free from this objection. For crystals containing more than one kind of atom Waller shows that the structure amplitude, obtained from the contributions from all the atoms which are in phase, is of the form $\sum F e^{-M}$ where F is the structure factor for an atom at rest. For face-centered cubic crystals M is given by

$$M = 8\pi^2 (\sin^2 \theta / \lambda^2) \bar{u}_{xx}^2, \quad (23)$$

where \bar{u}_{xx}^2 is the mean of the squares of the displacements in the x -direction for atoms of type κ from their mean positions. He finds that provided $T > \Theta/2\pi$ where Θ is the characteristic temperature of the crystal, \bar{u}_{xx}^2 is given by the equation

$$\bar{u}_{xx}^2 = \alpha_\kappa + \beta_\kappa + \gamma_\kappa/T + \delta_\kappa/T^3 + \dots \quad (24)$$

In (24) Waller shows that

$$\gamma_\kappa = \frac{1}{12m_\kappa} \left(\frac{h}{2\pi} \right)^2 \frac{1}{k}, \quad (25)$$

where m_κ is the mass of the atom, and h and k are Planck's and Boltzmann's constants, being thus independent of the atomic forces. He shows that δ_κ on the other hand depends on the atomic forces, but it is in a term whose value is very small and Waller and James²³ show that it can

be estimated with sufficient accuracy. Assuming zero-point energy equal to Planck's value, α_k in (24) is equal to zero, leaving β_k the only constant which cannot be calculated directly. However, Waller and James²³ show that a weighted mean given by the equation

$$\bar{\beta} = \sum m_k \beta_k / \sum m_k \quad (26)$$

can be determined with a fair degree of accuracy from a knowledge of the elastic constants of the crystal under investigation. From (23) and (24) they get for two different temperatures T_1 and T_2

$$\frac{\lambda^2}{8\pi^2 \sin^2 \theta} \{ (M_k)_1 - (M_k)_2 \} = \beta_k (T_1 - T_2) + \gamma_k \left(\frac{1}{T_1} - \frac{1}{T_2} \right) + \delta_k \left(\frac{1}{T_1^2} - \frac{1}{T_2^2} \right) + \dots \quad (27)$$

$$\bar{\beta} = \frac{k}{12(m_1 + m_2)} \left\{ \frac{(3\pi^2)^{\frac{1}{2}}}{\pi^2} \rho a^2 \frac{c_{44}(2c_{11} + c_{44}) + \frac{1}{2}b_1(c_{11} + c_{12})}{c_{11}c_{44}^2 + \frac{1}{2}b_1(c_{11} + c_{12})c_{44} + \frac{1}{16}b_1^2 b_2} + \frac{3}{\pi v_0^2} \right\} \quad (28)$$

In (28) $b_1 = c_{11} - c_{12} - 2c_{44}$, $b_2 = c_{11} + 2c_{12} + c_{44}$, and c_{11} , c_{12} and c_{44} are the elastic constants of the crystal in Voigt's notation.²⁴ Voigt obtained for rocksalt $c_{11} = 4.650 \times 10^{11}$, $c_{12} = 1.294 \times 10^{11}$, $c_{44} = 1.270 \times 10^{11}$. In (28), $v_0 (= c/\lambda_0)$ is the limiting frequency of the residual infrared rays which Havelock²⁵ has calculated to be 61.9μ from MacLaurin's²⁶ formula. In (28) ρ is the crystal density, 2.17 for rocksalt, and a the edge of the lattice, here 5.628Å. Thus $\bar{\beta}$ comes out 5.7×10^{-21} , in good agreement with the x-ray value above.

Waller and James show that the term involving δ is very small, even at liquid air temperatures, decreasing rapidly as T increases. From the two values of β for sodium and chlorine they proceed to determine M for each atom out of (28) and (23), finding for \bar{u}_{1z}^2 , chlorine, the value 0.0158×10^{-16} cm² and for \bar{u}_{2z}^2 the value 0.0196×10^{-16} cm². Now weighting the directions equally we have $\bar{u}_k^2 = 3\bar{u}_{kz}^2$ giving the mean square displacement of the chlorine atom 0.217Å and of

Now (27) should be constant for all values of θ for each kind of atom. Experimentally the mean of the left-hand side of (27) can be determined from all of the lines on a powder film for the two temperatures T_1 and T_2 (which should for accuracy be sufficiently wide apart) and thus β_k can be determined. By the use of rocksalt crystals at room temperature and at the temperature of liquid air they determined β_1 for chlorine to be 5.31×10^{-21} and β_2 for sodium to be 6.56×10^{-21} . Checking the centroid mean of these with the theoretical value obtained from elastic constants the agreement is remarkably good, the centroid mean being of course given by

$$\bar{\beta} = (m_1\beta_1 + m_2\beta_2)/(m_1 + m_2) = 5.8 \times 10^{-21}.$$

They show $\bar{\beta}$ to be given also by the equation involving the elastic constants of the crystal, *viz.*,

the sodium atom 0.242Å at room temperature (290°K). James and Firth,²⁷ using Fourier analysis, first introduced by Duane,²⁸ applied it to determine the change in electron distribution in the crystal with temperature thus getting for the mean displacement of the chlorine atom at room temperature 0.20Å and for the sodium atom 0.23Å, a remarkable agreement with the values of Waller and James considering that the method of James and Firth is equivalent to taking Planck's zero-point energy to be zero. For sylvine, KCl, James and Brindley²⁹ have determined β as 6.96×10^{-21} . But they found it impossible to determine M for chlorine and potassium separately since the diffracting powers of these are too nearly equal. They accordingly treated the atom of sylvine as simple cubic and took m in (28) as the mean of the masses of the atoms of chlorine and potassium. Thus for a simple cubic lattice with only one atom (28) reduces to

$$\beta = \frac{k}{3m} \frac{(6\pi^2)^{\frac{1}{2}}}{2\pi^2} \rho a^2 \frac{c_{44}(2c_{11} + c_{44}) + \frac{1}{2}b_1(c_{11} + c_{12})}{c_{11}c_{44}^2 + \frac{1}{2}b_1(c_{11} + c_{12})c_{44} + \frac{1}{16}b_1^2 b_2}, \quad (29)$$

in which James and Brindley have dropped the second term of the bracket in (28) without com-

ment, though the residual rays from sylvine differ not greatly from those from rocksalt. Their

value for the mean square displacement of sylvine is 0.255\AA at 290°K and 0.149\AA at 86°K .

In Fig. 8 we show the Debye temperature factor e^{-2M} for aluminum, copper, silver, gold, platinum, tungsten, lead and diamond. The values for the first five named are taken from Rusterholz,³⁰ for tungsten from Claassen.³¹ We have determined those for lead and diamond from known data for those elements. In all of the curves of Fig. 8 the zero-point energy

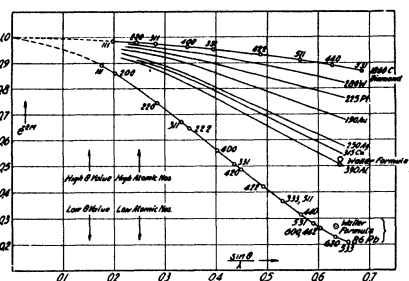


FIG. 8.

is included as given in (22). James, Waller and Hartree³² have verified the justification for zero-point energy. James, Brindley and Wood³³ have determined β in (27) for aluminum to be 3.218×10^{-21} and M from Waller's formula is $0.01182(h^2 + k^2 + l^2)$ for $T = 290^\circ$. If zero-point energy be dropped M is $0.00804(h^2 + k^2 + l^2)$. We have determined e^{-2M} for face 333 of aluminum, with zero-point energy. These points are shown in Fig. 8 for aluminum and lead. It is thus seen how close the agreement is between Debye's and Waller's formulas, the difference for face 620 in the case of lead, being 4 parts in 27 or 15 percent and for face 333 (511) of aluminum the error being 2 parts in 50 or 4 percent, zero-point energy being assumed in both formulas.

4. Absorption factor

A fourth factor affecting intensity is the absorption factor, one which has been known³⁴ for some time but which has been ignored by most experimenters except in special cases³⁵ until the year 1930 when Claassen's paper appeared.*

* Claassen, *The Calculation of Absorption in X-Ray Powder Photographs and the Scattering Power of Tungsten*, Phil. Mag. [7] 9, 57 (1930).

In Claassen's paper the absorption factor A , i.e., the ratio between the intensity of the diffracted beam and the intensity of the same beam without absorption is given as

$$A = (1/\pi r^2) \int e^{-\mu d} \cdot d\omega,$$

where d is the length of the ray through the powder sample, considered made up of strips, and μ is the linear absorption coefficient. Claassen states that this integral cannot be evaluated in the ordinary way but it can be solved graphically. For this purpose he divides the rod into strips of size $\Delta\omega$ such that rays diffracted by points in $\Delta\omega$ traverse a distance d between d and $d + \Delta d$ through the rod, giving approximately

$$A = (1/\pi r^2) \sum e^{-\mu d} \cdot \Delta\omega. \quad (30)$$

Claassen carries the division into strips out geometrically in the following way (Fig. 9). Call OI the incident beam axis and EO the reflected beam axis, the angle between these two axes being 2θ . Divide OI and EO up into tenths (Claassen used fifths) as indicated. From the points $0.4OI$ and $1.4EO$, say, draw two arcs of circles of radius r intersecting in S . Then the ray scattered in S has travelled a distance equal to $1.8r$ through the rod. Similarly any other two points, as $1.2OI$ and $0.6EO$, one on the incident ray (x_i) axis the other on the reflected ray (x_r) axis, and adding up to $1.8r$ as measured along these axes, determine a point scattering a ray that travels $1.8r$ through the rod. In this way the curves $PSS'Q$ and $MS''N$ are obtained. Thus as shown in Fig. 9, for the case where $\theta = 22.5^\circ$, all points on MN and PQ scatter x-rays whose

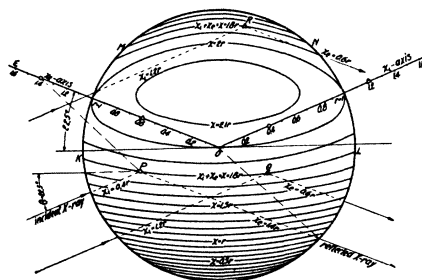


FIG. 9.

length of path through the rod is 1.8 times the radius. Claassen calls the points along the curves PQ and MN for shortness "points 1.8r" and in general all such points "points a ." Constructing the loci for several values of a , the size of the strips $\Delta\omega$ belonging to these values of a are obtained by measuring their area with a planimeter. Putting $x=d/r$ in (30) the area, Δs , expressed in terms of the total area of the sample as unity, contains all points from x to $x+\Delta x$ and is a function of x only. Hence (30) becomes

$$A = \sum e^{-\mu r x} \cdot \Delta s. \tag{31}$$

Claassen presents a table connecting x and Δs for variations of x of 0.2 from 0 to 3.8, the values

of θ varying from 0° to 90° by steps of 22.5° . We have reduced the steps for both θ and Δx by half. Fig. 9 shows, for $\theta=22.5^\circ$, the strips of cross-sectional area which were measured to determine $\Delta\omega$, from which Δs was then calculated. These values of Δs are shown in Table II. With the formula

$$A(\theta) = \sum e^{-\mu r(x+\frac{1}{2}\Delta x)} \cdot \Delta s \tag{32}$$

the first seven curves of Fig. 10 for $\mu r=0.2, 0.4, 0.6, 0.8, 1.0, 1.5, 2.0$ were plotted from the graphical integrations (Table II).

As shown below from the work of Rusterholz²⁰ for very large values of μr the value of $A(\theta)$ by integration is given by

$$A(\theta) = \frac{r_0}{\mu} \left\{ 1 + \frac{\cos^2 \theta}{2 \sin \theta} \log_e \left[\frac{\cos 2\theta + \sin \theta}{(1 + \sin \theta)(1 + 2 \sin \theta)} \right] \right\}. \tag{47}$$

TABLE II.

$x + \frac{1}{2}\Delta x$	$\theta=0^\circ$	11.25°	22.5°	33.75°	45°	56.25°	67.5°	78.75°	90°
0.05	00.01	00.18	00.33	00.81	1.18	1.75	2.20	3.02	3.27
15	0.04	0.23	0.41	0.87	1.56	2.00	2.68	3.03	3.24
25	0.10	0.30	0.66	0.94	1.72	2.18	2.73	3.05	3.21
35	0.19	0.40	0.84	1.07	1.77	2.35	2.78	3.07	3.18
45	0.32	0.53	0.97	1.48	1.82	2.53	2.83	3.08	3.16
55	0.47	0.66	1.15	1.65	2.08	2.66	2.89	3.10	3.14
65	0.70	0.81	1.33	1.83	2.26	2.76	2.96	3.11	3.12
75	0.96	1.04	1.50	2.04	2.46	2.84	3.02	3.12	3.10
85	1.29	1.39	1.74	2.26	2.64	2.91	3.07	3.11	3.08
95	1.62	1.75	1.91	2.47	2.80	3.01	3.12	3.10	3.06
1.05	2.06	2.13	2.17	2.70	2.92	3.14	3.17	3.09	3.04
15	2.51	2.59	2.42	2.92	3.13	3.27	3.22	3.08	3.02
25	3.11	3.12	2.83	3.18	3.33	3.37	3.27	3.07	3.00
35	3.82	3.80	3.16	3.46	3.49	3.47	3.32	3.05	2.98
45	4.77	4.64	3.55	3.77	3.69	3.57	3.35	3.03	2.96
55	6.05	5.63	4.67	4.15	3.90	3.65	3.30	3.01	2.93
65	7.75	7.05	5.79	4.50	4.13	3.70	3.25	2.98	2.90
75	10.10	9.33	7.20	5.04	4.33	3.75	3.20	2.95	2.87
85	14.57	12.93	8.91	5.60	4.64	3.77	3.17	2.92	2.84
95	39.56	23.87	13.34	7.05	4.92	3.80	3.12	2.88	2.80
2.05		17.62	20.15	8.45	5.13	3.75	3.09	2.84	2.75
15			14.97	9.80	5.23	3.70	3.04	2.79	2.70
25				11.07	5.25	3.65	2.99	2.73	2.65
35				11.09	5.21	3.57	2.94	2.66	2.60
45				0.92	5.13	3.49	2.87	2.58	2.54
55					5.00	3.39	2.68	2.50	2.48
65					4.62	3.27	2.58	2.42	2.42
75					4.42	3.12	2.50	2.34	2.35
85					1.24	2.94	2.41	2.26	2.27
95						2.73	2.31	2.18	2.16
3.05						2.40	2.14	2.10	2.06
15						1.95	1.96	2.01	1.95
25						1.39	1.75	1.91	1.83
35						0.17	1.40	1.79	1.70
45							1.10	1.64	1.56
55							0.64	1.46	1.41
65								1.24	1.25
75								0.97	1.07
85								0.73	0.85
95									0.50

Between this limiting value of $A(\theta)$ and the values given by (32) Claassen shows it is possible to obtain $A(\theta)$ by a series method for values of x less than 1. Call $f(x)$ the area containing all

points less than x . Taking $f(x)$ as a power series

$$f(x) = \alpha x + \beta x^2 + \gamma x^3 + \delta x^4 + \dots \tag{33}$$

we have $ds = (df/dx)dx$, whence

$$A = \int e^{-\mu r x} \cdot (df/dx)dx \tag{34}$$

$$= \int e^{-\mu r x} \cdot (\alpha + 2\beta x + 3\gamma x^2 + \dots)dx.$$

Integrating from 0 to ∞ , which is permissible for μ large gives

$$A = \frac{1}{\mu r_0} \left(\alpha + \frac{2\beta}{\mu r_0} + \frac{6\gamma}{\mu^2 r_0^2} + \dots \right), \tag{35}$$

where r_0 is the sample radius expressed in cm. Claassen tabulates the coefficients α, β and γ for 22.5° steps. These are shown plotted in Fig. 11. Our values for these coefficients are also shown in the figure.

When Table II is plotted the graphs of Fig. 12 are obtained. Slight errors in the planimeter work in getting areas are ironed out in the figure. It is rather interesting to note the way in which the various curves cross one another. In Eq. (34) for large values of μ $e^{-\mu r x}$ changes rapidly, $A(\theta)/A(90)$ having of course the maximum slope

for $\mu r_0 = \infty$ as shown by Fig. 10. On the other hand, Fig. 12 shows that Δs changes most rapidly for θ zero and least rapidly for $\theta = 90^\circ$. It is noticeable that the curves of Fig. 12 have, roughly speaking, a common point of intersection for $(x + \frac{1}{2}\Delta x) = 1.25$ which is not much above the value 1 taken by Claassen as the range of validity of the series (35). In getting our values of β and γ , the graphical integration was used for values of $x + \Delta x/2$ equal to 1.15 on down. Plotting the values of β and γ against x gives the curves of Fig. 13. It is noticed at once that for all values of θ except 67.5 the slopes of the curves for values of x between 1.0 and 1.2 are changing

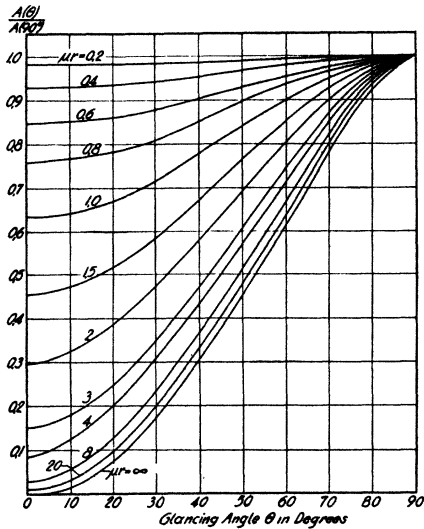


FIG. 10.

very slowly. Hence by choosing our values of β and γ plotted in Fig. 13 for $x = 1.1$ the errors will be very small. For $\theta = 67.5^\circ$ the slope appears to be considerable. However, using the slope as given by the curves for this angle we are able to get smooth β and γ curves. A good test of the choice of β and γ values used can be found by comparing the series and the graphical integrations for values of μr_0 between 3 and 8. Practically perfect agreement is found. Thus Fig. 10 is seen to be correct throughout its entire range. There is also complete agreement between our

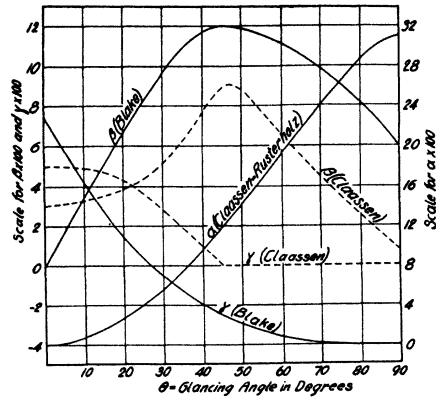


FIG. 11.

series values and Rusterholz' graphical values for $\mu r_0 = 5.24$ and 8.56 . (Compare Fig. 20.) There are, in fact, two principal reasons for not exceeding $x = 1.1$ in determining the proper values of β and γ in our power series. First, for $\mu r_0 > 4$ the values of $e^{-\mu r(x + \frac{1}{2}\Delta x)}$ for values of $x > 1.1$ are practically negligible and although Δs is increasing rapidly for values of θ below 33.75° for values of $x > 1.1$ the product $e^{-\mu r x} \cdot \Delta s$ is still negligible as compared to the same product for lower values of x . Second, Fig. 12 shows clearly that below $x = 1.1$ the slope of each of the several Δs curves for different values of θ is essentially constant, whereas for larger values of x than 1.1 the slope for certain curves is varying rapidly. We arbitrarily took $\beta = 0$ for $\theta = 0$ instead of using the value -0.005 as given from Fig. 13 for the reason that a negative value of β for μr_0 large makes A

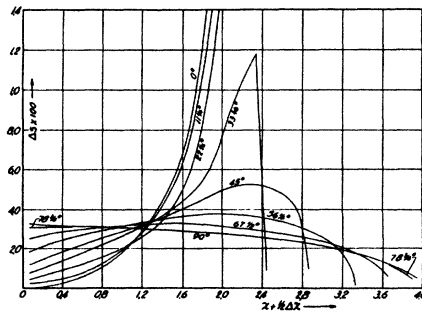


FIG. 12.

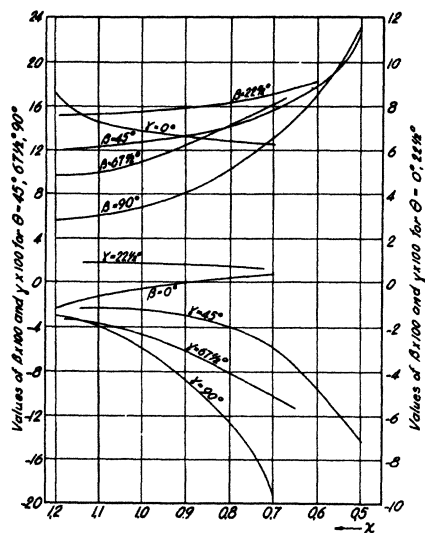


FIG. 13.

negative, which is impossible. As a matter of fact for $\theta=0$ it is incorrect, in getting $e^{-\mu r x} \cdot \Delta s$, to stop at $x=1.1$ for the reason that the values of Δs for x small are exceedingly small while Δs for x large is very large. The negative value -0.005 , obtained on stopping at $x=1.1$, is accordingly itself wrong. By taking β zero for θ zero (α being zero here) we make the series valid for values of $\mu r > 10$ and introduce thereby only inappreciable error in the series for values of μr below 10. Below $\mu r = 4$ the series breaks down and above $\mu r = 8$ the graphical integration breaks down for the reason that Δx is not taken small enough.

Since Rusterholz obtained his values of α by integration for large values of μr_0 it necessarily agrees with Claassen's values except in very minor differences. Our curves for β and γ differ from Claassen's in two respects, their shapes are different for low values of θ , while for higher values of θ our values of β are about as much

above his as our values of γ are below his. Claassen deemed it expedient not to use negative values of γ whereas negative values become necessary for $\theta > 26.5^\circ$ in order to make the graphical integration agree with the series integration for intermediate values of μr_0 , viz., those between 2 and 8.

Rusterholz²⁰ starts with the Debye-Compton formula, obtained by considering the coherent scattering of unpolarized x-rays from an element dV of crystal powder, viz.,

$$\frac{I}{I_0} = C n^2 |S|^2 p \frac{1 + \cos^2 2\theta}{\sin 2\theta \sin \theta} \frac{dV}{r} \quad (36)$$

In this formula one recognizes at once the polarization factor, the Lorentz factor for powders, and the square of the structure factor, p being the form or multiplicity factor n the number of atoms per unit volume, r the distance from the element of volume dV irradiated to the photographic film, I the reflected intensity and I_0 the primary intensity.

If absorption within the body of material irradiated is neglected formula (36) may be written

$$I/I_0 = f(r, \theta) dV. \quad (37)$$

If the primary ray penetrates the distance s_1 through the volume dV and the reflected ray the distance s_2 then, allowing for absorption, one must put

$$I/I_0 = f(r, \theta) \int e^{-\mu(s_1+s_2)} \cdot dV. \quad (38)$$

If now in the Debye-Scherrer powder method the sample be taken as cylindrical of height h and of cross-sectional area $d\omega$ one can put for $\int e^{-\mu(s_1+s_2)} \cdot dV$ the expression $h \int e^{-(s_1+s_2)} \cdot d\omega \equiv hA(\theta)$ provided h is small compared to the radius of the camera and the primary beam is parallel or not too divergent.

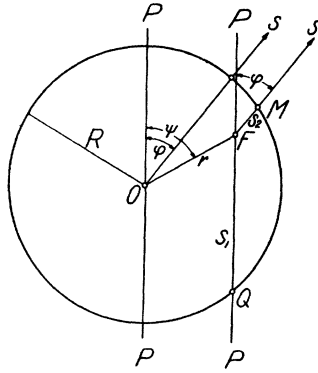


FIG. 14.

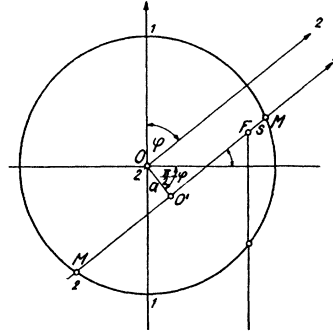


FIG. 15.

If the cross section of the sample is circular of radius r_0 the formula for A becomes

$$A(\theta) = \int_0^{r_0} \int_0^{2\pi} e^{-\mu r} \left[\left\{ 1 - \frac{r^2}{r_0^2} \sin^2(\psi - \phi) \right\}^{\frac{1}{2}} + \left\{ 1 - \frac{r^2}{r_0^2} \sin^2 \psi \right\}^{\frac{1}{2}} - \frac{r}{r_0} \cos(\psi - \phi) + \frac{r}{r_0} \cos \psi \right] r dr d\psi \quad (39)$$

for by inspection of Fig. 14 it is seen that

$$s_1 = y_1 + y_2 = r_0 \left[\left\{ 1 - \frac{r^2}{r_0^2} \sin^2 \psi \right\}^{\frac{1}{2}} + \frac{r}{r_0} \cos \psi \right]$$

and

$$s_2 = r_0 \left[\left\{ 1 - \frac{r^2}{r_0^2} \sin^2(\psi - \phi) \right\} - \frac{r}{r_0} \cos(\psi - \phi) \right].$$

Now in general this integral cannot be calculated analytically. But in special cases it has been determined either graphically or by numerical methods. By putting $r = r_1 r_0$ and $\mu r_0 = \mu_1$ the integral can be expressed as

$$A(\theta) = r_0^2 \int_0^1 \int_0^{2\pi} e^{-\mu_1 [(1-r_1^2 \sin^2(\psi - \phi))^{\frac{1}{2}} + (1-r_1^2 \sin^2 \psi)^{\frac{1}{2}} - r_1 \cos(\psi - \phi) + r_1 \cos \psi]} \cdot r_1 dr_1 d\psi. \quad (40)$$

If (see Fig. 15) P is the primary and S the secondary ray and F the position of a small crystal from which the secondary ray is reflected, this ray cutting the circumference of the sample in the two points MM' , then, if the cartesian coordinates of M are x, y and if the distance from the center of the sample to the line MM' is a , we have from geometry

$$x_1 = a \cos \phi + (1 - a^2)^{\frac{1}{2}} \sin \phi \quad \text{and} \quad y_1 = (1 - x_1^2)^{\frac{1}{2}}.$$

Calling the distance $FM = s$, the coordinates of F being x, y we have $x = x_1 - s \sin \phi$ and $y = y_1 - s \cos \phi$, giving finally the distance $s_1 + s_2$ traversed by the ray through the material to be

$$s_1 + s_2 = y + (1 - x^2)^{\frac{1}{2}} + s. \quad (41)$$

Integrating over all elements of surface lying on the straight line MM' we get

$$A(\theta) = r_0^2 \int_{-1}^{+1} da \int_M^{M'} e^{-\mu_1 (y + (1 - x^2)^{\frac{1}{2}} + s)} \cdot ds = r_0^2 \int_{-1}^{+1} I(a, \phi) da, \text{ say.} \quad (42)$$

Here it is to be remembered that in Figs. 14 and 15, $\phi = 2\theta$.

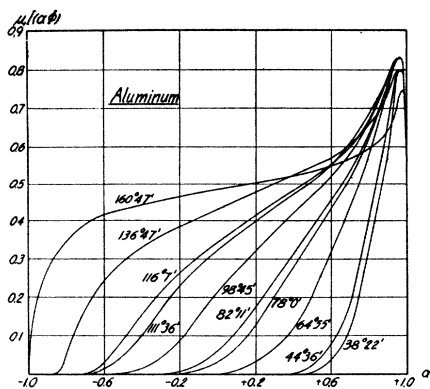


FIG. 16.

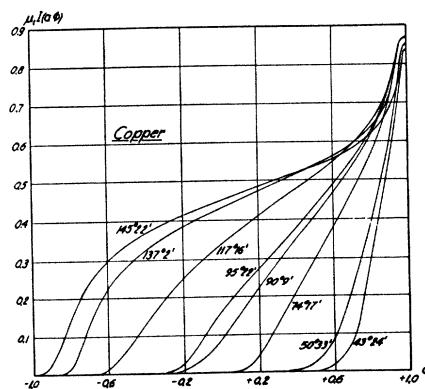


FIG. 17.

But again this integral in general cannot be determined except by methods of approximation so we choose Δs small enough that the substitution of a summation for the integration introduces an error not greater than $\frac{1}{2}$ percent, say. Thus

$$I(a, \phi) = \sum e^{-\mu_1(\nu_i + (1-z_i^2)^{1/2} + s_i)} \cdot \Delta s_i \quad (43)$$

The larger μ_1 is the smaller I becomes, reaching finally a limiting value.

Using the mass absorption coefficients given by Jönsson for Al and Cu for copper, $K\alpha$ -rays, Rusterholz† determines the values of I for the first ten lines of Al and for the first eight lines of copper. Multiplying his tables for I by μ_1 he gives the curves $\mu_1 I(a, \phi)$ as a function of a from -1 to $+1$, which are here reproduced as Figs. 16 and 17. Taking the areas under the curves gives the values of $A(\theta)/A(90)$ given in the following table, Table III.

TABLE III.

Aluminum				Copper			
Face (Rusterholz)	2θ (Blake)	2θ	$A(\theta)/A(90)$	Face (Rusterholz)	2θ (Blake)	2θ	$A(\theta)/A(90)$
111	38°22'	38°30'	0.144	111	43°24'	43°22'	0.133
200	44°36'	44°45'	0.174	200	50°33'	50°31'	0.172
220	64°55'	65° 8'	0.297	220	74°17'	74°13'	0.319
311	78° 0'	78°17'	0.382	311	90° 9'	90° 4'	0.427
222	82°11'	82°30'	0.406	222	95°22'	95°17'	0.469
400	98°45'	99°10'	0.532	400	117°16'	117° 8'	0.646
331	111°36'	112° 7'	0.635	331	137° 2'	136°49'	0.802
420	116° 7'	116°41'	0.659	420	145°22'	145° 6'	0.857
422	136°44'	137°38'	0.815		180°	180°	1.000
333	160°47'	162°59'	0.948				
511	180°	180°	1.000				
	$a = 4.047$	$a = 4.0438$			$a = 3.607$	$a = 3.6080$	
	about likely				likely		

Again Rusterholz takes (Fig. 18) a small crystal surface at F , POP being the primary ray and FM the secondary ray. In the expression for $I(a, \phi)$ given in (42) viz.,

$$I(a) = \int_M^{M'} e^{-\mu_1(s_1 + s_2)} \cdot ds.$$

Rusterholz takes s_2 to be small for large values of μ_1 and integrates from 0 to ∞ instead of from M to M' obtaining thus

$$I(a) = \int_0^\infty e^{-\mu_1 s_2 [1 + \sin \alpha / \sin (2\theta - \alpha)]} \cdot ds, \quad (44)$$

since from the figure we have

$$s_1/s_2 = \sin \alpha / \sin (2\theta - \alpha).$$

Thus he gets

$$I(a) = \frac{1}{\mu_1} \left\{ \frac{\sin (2\theta - \alpha)}{\sin (2\theta - \alpha) + \sin \alpha} \right\} \quad (45)$$

for $\cos 2\theta \leq a \leq +1$, $I(a)$ being zero for $a < \cos 2\theta$.

† Rusterholz used a camera of 8 cm diameter and was aware that the radius of the sample, for good technique, had to be small compared to the radius of the camera. If μ/ρ for Al is 51.2 and $\rho = 2.7$ and μ/ρ for Cu is 50.4 and $\rho = 8.9$, μr_0 being 5.24 for Al and 8.56 for Cu we get the values of r_0 used by Rusterholz to be 0.38 mm for Al and 0.19 mm for Cu. The larger of these values is less than 1 percent of the camera radius. Inadvertently his Tables V and VI have $A(\phi)$ instead of $A(\phi)/A(\pi)$ as one of the headings.

In this way Rusterholz plots $\mu_1 I(a, \phi)$ against a , reproduced here as Fig. 19. Thus, finally,

$$A(\theta) = \frac{r_0^2}{\mu_1} \int_{\cos 2\theta}^{+1} \frac{\sin(2\theta - \alpha)}{\sin(2\theta - \alpha) + \sin \alpha} da = \frac{r_0^2}{\mu_1} \int_0^{2\theta} \frac{\sin(2\theta - \alpha) \sin \alpha}{\sin(2\theta - \alpha) + \sin \alpha} d\alpha, \quad (46)$$

since $a = \cos \alpha$. Rusterholz points out that Claassen derived (46) in another way. He shows that (46) can be integrated directly, whereas Claassen thought it could be integrated only by graphical or numerical methods. His result is

$$A(\theta) = \frac{r_0}{\mu} \left\{ 1 + \frac{\cos^2 \theta}{2 \sin \theta} \log_e \left[\frac{\cos 2\theta + \sin \theta}{(1 + \sin \theta)(1 + 2 \sin \theta)} \right] \right\}. \quad (47)$$

This reduces to r_0/μ when $\theta = \pi/2$. This limiting value is, of course, a maximum value for $A(\theta)$ as shown by Fig. 10.

Rusterholz plots $A(2\theta)/A(\pi)$ for three different values of μr_0 , viz., 5.24, 8.56 and 50 ($= \infty$), reproduced as Fig. 20. As shown by a note in this survey (p. 183) the first two values are for aluminum and copper but the radius of his aluminum sample was twice what it was for copper. His value for $\mu r_0 = 50$ differs appreciably from that for $\mu r_0 = \infty$ as will be shown later. The reader should remember that curves like those of Fig. 20 are legitimate when changing either μ or r_0 provided the maximum value of r_0 used is small compared to the camera radius and provided μr_0 is large enough for Eqs. (45) to (47) to hold. This proviso must, of course, be critically inspected in any given case.

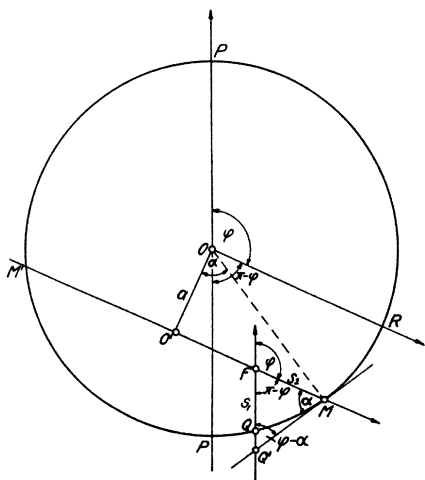


FIG. 18.

Greenwood²⁵ obtained values of $A(\theta)$ differing greatly from those of Claassen and Rusterholz. The latter concludes that Greenwood has made errors in his calculations and assigns this as the reason why Greenwood's values for the atomic scattering factor for aluminum differs from the experiments of Bearden,²⁶ and of James, Brindley and Wood.²⁷

Because of taking $\mu r_0 > 50$ for Ag, Pt and Au, Rusterholz obtains values of $A(\theta)$ for these metals that lie upon the same curve when plotted against $\sin \theta/\lambda$. The curves for these three metals practically superpose upon the values given by Claassen for tungsten, except for the larger values of $\sin \theta/\lambda$. In Fig. 21 all the curves for the five metals used by Rusterholz and Claassen's curve for tungsten are shown. Since the reciprocal of 1.539 is 0.65 all these curves must converge to

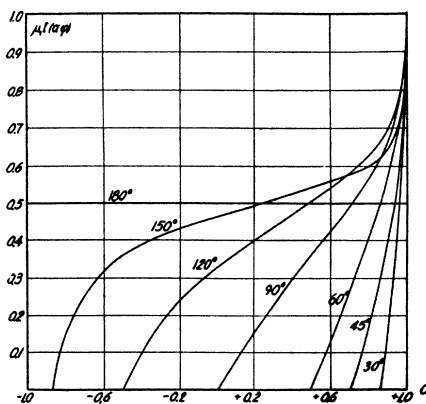


FIG. 19.

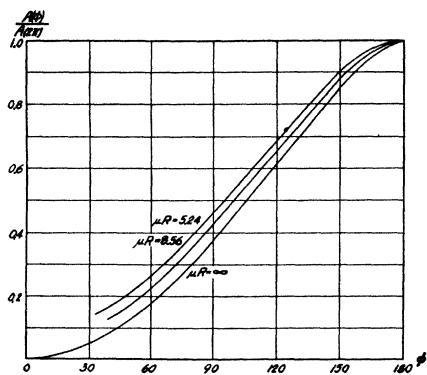


FIG. 20.

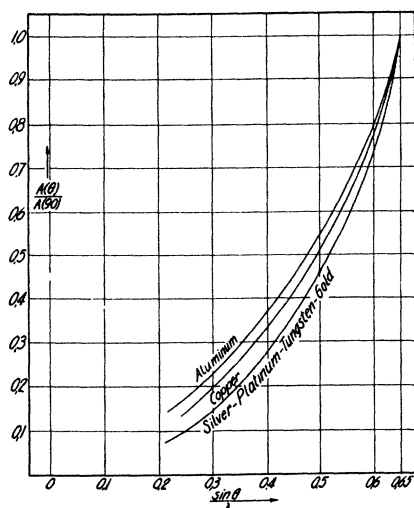


FIG. 21.

unity for $A(\theta)$ for that value of $\sin \theta/\lambda$, since both Claassen and Rusterholz have calculated $A(\theta)$ for copper $K\alpha$ -rays only.

It will be shown later in this paper that the changes in $A(\theta)$ as $\sin \theta/\lambda$ increases for molybdenum $K\alpha$ -rays are very much less than for copper rays. But it is obvious from the curves of Fig. 20 that if A is taken as unity for the 111 face of aluminum, say, the change in A as θ increases, keeping λ constant, is 660 percent, while for silver it is 1250 percent. Thus this A factor far transcends both the Debye factor and

the atomic form factor (to be spoken of shortly) and works in the opposite direction from each of these. And yet up to date this factor has for the most part been ignored by the x-ray analysts. Fortunately for crystal structure determination, most of the crystals studied to date have been made using molybdenum or other rays shorter than copper rays where the effect is less, otherwise a good deal of crystal structure determinations would have to be made over.

5. Structure factor

The next factor to take into account is the so-called atomic structure factor usually represented by S . Consider two interpenetrating rows of atoms as shown in Fig. 22. The straight line

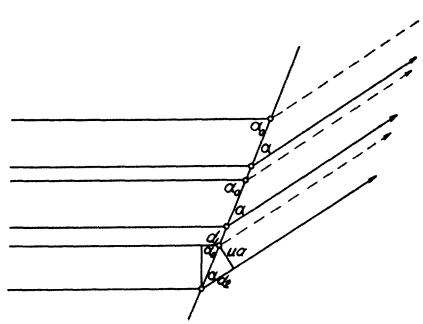


FIG. 22.

passing through the points makes the angle α_0 with the primary ray and the angle α with the secondary rays, the secondary rays emanating from the second type of atom being dotted. If the distance between the secondary rays emitted by the two types of atoms be taken as ua , then the difference in path between the secondary rays from the two types of atoms is given as $d_2 - d_1 = ua(\cos \alpha - \cos \alpha_0) = xh\lambda$, say. Since, however, the interferences from the two types of atoms have different amplitudes we must add the two waves, thus:

$$y = A_1 \cos 2\pi(r/\lambda - t/\tau) + A_2 \cos 2\pi(r/\lambda - t/\tau + xh). \quad (48)$$

Representing these waves in the exponential form we get

$$y = (A_1 + A_2 e^{2\pi i x h}) e^{2\pi i(r/\lambda - t/\tau)}. \quad (49)$$

The parenthesis in this expression is called the structure factor S . Had we been dealing with two *volume* gratings instead of two *line* gratings the parenthesis would have taken the form

$$S = A_1 + A_2 e^{2\pi i(xh + yk + zl)}$$

Again if there were not two gratings only that interpenetrated but any number it is obvious that S would be given by the equation

$$S = \sum A_r e^{2\pi i(x_r h + y_r k + z_r l)} \quad (50)$$

Here x_r, y_r, z_r is the position of the r th atom in the unit cell and h, k, l , are whole numbers, the so-called Miller indices. If one draws the axial vectors $\mathbf{a}, \mathbf{b}, \mathbf{c}$ then from Fig. 23 it is clear that

$$\mathbf{r}_r = x_r \mathbf{a} + y_r \mathbf{b} + z_r \mathbf{c}$$

But from our knowledge of the reciprocal grating we know that

$$|\mathbf{h}| = |h\mathbf{a}^* + k\mathbf{b}^* + l\mathbf{c}^*|$$

and that

$$\left. \begin{aligned} (\mathbf{a}\mathbf{a}^*) &= (\mathbf{b}\mathbf{b}^*) = (\mathbf{c}\mathbf{c}^*) = 1 \\ (\mathbf{a}\mathbf{b}^*) &= (\mathbf{b}\mathbf{c}^*) = (\mathbf{c}\mathbf{a}^*) = 0 \\ (\mathbf{a}^*\mathbf{b}) &= \mathbf{b}^*\mathbf{c} = (\mathbf{c}^*\mathbf{a}) = 0 \end{aligned} \right\}$$

and these taken together give

$$(\mathbf{r}, \mathbf{h}) = x_r h + y_r k + z_r l,$$

whence

$$S = \sum Z_r e^{2\pi i(\mathbf{r}, \mathbf{h})} = \sum Z_r e^{2\pi i(x_r h + y_r k + z_r l)} \quad (51)$$

which is (50) where Z_r , the atomic number, is substituted for the amplitude A_r .

S is in general complex and it may accordingly be evaluated in the customary manner by multiplication with its conjugate complex giving

$$|S|^2 = \sum_r \sum_s Z_r Z_s e^{2\pi i[(x_r - x_s)h + (y_r - y_s)k + (z_r - z_s)l]}$$

which must, of course, be real. Taking the real part we get

$$|S|^2 = \sum_r \sum_s Z_r Z_s \cos 2\pi[(x_r - x_s)h + (y_r - y_s)k + (z_r - z_s)l],$$

which, when written vectorially takes the form

$$|S|^2 = \sum_r \sum_s Z_r Z_s \cos 2\pi(\mathbf{r}_r - \mathbf{r}_s, \mathbf{h}) \quad (52)$$

Now this formula for the structure factor assumes that all the planetary electrons within each atom reinforce one another in the matter of their x-ray interferences as if they all had the same phase. But this is far from true. Rather we must determine these phase relations. This has been done by Debye in the following way, with notation after v. Laue.

6. Atomic form factor

Consider an atom supposed to scatter like a point source. If \mathbf{S}_0 is a unit vector in the direction of the primary radiation and \mathbf{S} such a vector in the direction of observation of the scattered radiation, then if A is the amplitude of the incident radiation the scattered radiation at a point P distant R from the atom in the direction \mathbf{S} will be proportional to $(A/R)e^{i\omega t} \cdot e^{-k(\mathbf{S}_0 \cdot \mathbf{r})} \cdot e^{-ikR}$, where

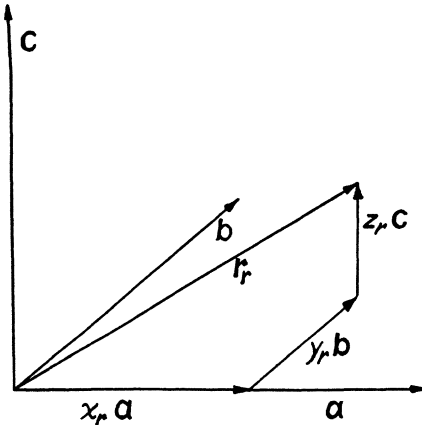


FIG. 23.

\mathbf{r} is the vector distance from the origin of coordinates to the atom (see Fig. 24). In this equation ω is 2π times the frequency of the x-radiation and $k=2\pi$ divided by the wavelength. Since R is always large one can say that $R=R_0-(\mathbf{r}\cdot\mathbf{S})$, very approximately. Introducing a proportionality factor f , we have as the amplitude at P

$$[fAe^{i(\omega t-kR_0)/R_0}] \cdot e^{ik(\mathbf{S}-\mathbf{S}_0)\cdot\mathbf{r}}. \quad (53)$$

Dropping the factor $e^{i(\omega t-kR_0)/R}$ which is common to all progressive waves and remembering that in any triangle of vectors formed on the two sides \mathbf{S}_0 and \mathbf{S} the vector $\mathbf{S}-\mathbf{S}_0=\mathbf{s}$, the third side, our scattered amplitude at P becomes $fAe^{ik(\mathbf{s}\cdot\mathbf{r})}$. We must now sum this expression for

all n atoms of the same kind giving the amplitude $i\sum f_i A e^{ik(\mathbf{s}\cdot\mathbf{r}_i)}$. Since the intensity I is proportional to the square of the amplitude we can say that

$$I = A^2 \sum_i \sum_j f_i f_j e^{ik(\mathbf{s}\cdot\mathbf{r}_{ij})}, \quad (54)$$

where \mathbf{r}_{ij} is the vector $\mathbf{r}_i - \mathbf{r}_j$. Now an atom may exist anywhere on a zone of equal probability on a sphere of radius $r_{ij}=l$, say (see Fig. 25), and we must seek the average value of $e^{ik(\mathbf{s}\cdot\mathbf{r}_{ij})}$. This average value is $[\int e^{iksl \cos \theta} \cdot d\omega] / \int d\omega$, where $d\omega$ is an element of surface on the sphere. Substituting in the numerator for $d\omega$ the zonal area $2\pi \sin \theta d\theta$ and carrying out the integration in the denominator the average value becomes

$$\left[\int e^{iksl \cos \theta} \cdot 2\pi \sin \theta d\theta \right] / 4\pi = -\frac{1}{2} \int_{-1}^{+1} e^{iksl \cos \theta} \cdot d(\cos \theta) = \sin ksl / ksl. \quad (55)$$

In this expression ksl is equal to $(4\pi ls \sin \theta) / \lambda = x$, say.

If now we seek the atomic form factor for an atom we must calculate the interferences due to the various planetary electrons in the atom by calculating the probability that an electron finds itself in a certain element of volume dv . Let udv

be this probability. Putting our origin at the nucleus of the atom and considering its electron cloud as possessing spherical symmetry, we denote by \mathbf{r} the radius vector to the element of volume dv , by S_0 the amplitude of the incident radiation and by S the amplitude of the scattered radiation. Then the third side of the vector triangle is $\mathbf{s}=\mathbf{S}-\mathbf{S}_0$. The scattering amplitude f is then given by the following relation

$$f \propto \int e^{ik(\mathbf{s}\cdot\mathbf{r})} \cdot u dv, \quad \text{where } k=2\pi/\lambda.$$

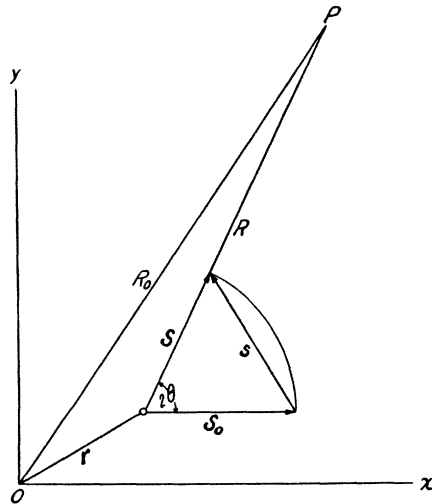


FIG. 24.

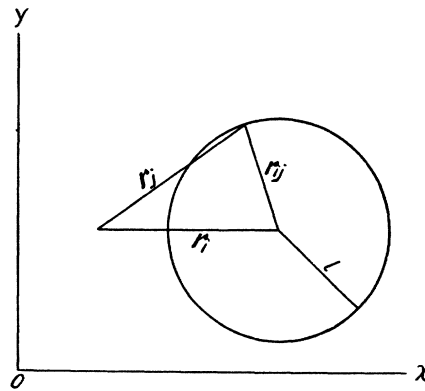


FIG. 25.

For λ increasing the phase difference between the wavelets scattered by the different electrons within the atom differ less and less until the integral becomes unity and f equals the atomic number. In general then we have

$$f^2 = \left(\frac{a_e}{R}\right)^2 \frac{1 + \cos^2 2\theta}{2} \left| \int e^{ik(\mathbf{s}\cdot\mathbf{r})} \cdot u d\mathbf{v} \right|^2. \quad (56)$$

Calling the absolute value of the integral F we have

$$f^2 = (a_e/R)^2 [(1 + \cos^2 2\theta)/2] F^2(u).$$

Here a_e can be called the "radius of the electron" and is equal to $e^2/mc^2 = 3 \times 10^{-13}$ cm obtained from the Thomson classical formula for scattering

$$\frac{I}{I_0} = \left(\frac{e^2}{mc^2}\right)^2 \cdot \frac{1 + \cos^2 2\theta}{2}. \quad (57)$$

Taking the element of volume $d\mathbf{v}$ to be that of a zone of latitude of width $r d\alpha$ and of thickness dr , we have

$$\begin{aligned} F(u) &= 2\pi \int_0^\infty e^{ik(\mathbf{s}\cdot\mathbf{r})} \cdot u(r) r^2 dr \int_0^\pi \sin \alpha d\alpha \\ &= 4\pi \int_0^\infty u(r) r^2 dr (\sin ksr / ksr) \end{aligned} \quad (58)$$

on account of (55) where r is substituted for l .

Now we can identify $u(r)$ with $|\psi|^2$ where ψ is the Schrödinger wave function. It is known that ψ for the hydrogen atom (having one electron), for instance, is given by

$$\psi = e^{-r/a_H} / (\pi a_H^3)^{1/2}, \text{ where } a_H = \hbar^2 / 4\pi^2 m e^2 = 0.532 \text{ \AA}.$$

Inserting the value of u and calling $r/a_H = \rho$ we have

$$F(u) = 4 \int_0^\infty e^{-2\rho} \cdot \rho^2 \cdot \frac{\sin u\rho}{u\rho} \cdot d\rho = \frac{1}{(1 + u^2/4)^2}, \quad (59)$$

where

$$u = k s a_H = (4\pi a_H / \lambda) \sin \theta. \quad (60)$$

Now in seeking the atomic form factor for any sort of atom we recall that the probability of finding the electron in a certain location is given by the square of the Schrödinger wave function.

Now the energy of the hydrogen atom is given by

$$E = (1/2m)(p_x^2 + p_y^2 + p_z^2) - e^2/r,$$

Inserting the prescription $p = (\hbar/2\pi i) \partial/\partial x$ and also the wave function ψ we get

$$(1/2m)(\hbar/2\pi i) \nabla^2 \psi - e^2 \psi / r = \psi E. \quad (61)$$

Now from wave-mechanical theory it is known that ψ is everywhere finite and that E has only certain discrete values.

Put $\psi = C e^{-\alpha r}$ in (61) and we get

$$(\alpha^2 - 2\alpha/r) + (8\pi^2 m / \hbar^2)(E + e^2/r) = 0. \quad (62)$$

For this Eq. (62) to be everywhere true we must have the coefficient of $1/r$ equal to zero, giving

$$\alpha = 4\pi^2 m e^2 / \hbar^2 = 1/a_H \text{ and } E = -2\pi^2 m e^4 / \hbar^2.$$

But the probability that the electron of the hydrogen atom finds itself somewhere in the neighborhood of the hydrogen nucleus is a certainty, giving

$$\int \psi^2 d\mathbf{v} = \int C^2 e^{-2\alpha r} \cdot d\mathbf{v} = 1,$$

from which we find

$$C = 1/(\pi a_H^3)^{1/2}. \quad (63)$$

Now if Φ is the average value of the electrostatic potential of the hydrogen atom we have as the expression of the energy $(p_x^2 + p_y^2 + p_z^2)/2m - e\Phi$. Making two of the p 's zero and dropping the subscript on the third we get as the condition for the electron belonging to the atom that $p^2/2m \leq e\Phi$, hence the largest value possible for p is given by $p = (2me\Phi)^{1/2}$. Now in phase space p can be taken as the radius of a sphere and the element of volume $d\mathbf{v}$ can be taken as the volume of a sphere of this radius. But in wave mechanics it is known that the smallest permissible volume (i.e., unit cell) is h^3 . Since according to Pauli's principle there can be only one electron per cell, we get for the number ν of electrons in the element $d\mathbf{v}$,

$$\nu d\mathbf{v} = (2/\hbar^3) \cdot (4\pi/3) (2me\Phi)^{3/2} d\mathbf{v},$$

the 2 being inserted on account of the double sign of the electron spin. We get finally the number of electrons per unit volume of phase space to be

$$\nu = (8\pi/3\hbar^3) (2me\Phi)^{3/2}. \quad (64)$$

But Poisson's equation holds for the electrostatic potential, viz., $\Delta\Phi = 4\pi\nu e$ and inserting the value of ν given by (64) we get

$$\Delta\Phi = (32\pi^2/3)e(2me/h^2)^{1/2}\Phi^{1/2} = k\Phi^{1/2}, \text{ say.} \quad (65)$$

Professor Debye remarks that the method here used corresponds exactly to the one used in determining the ionic cloud in electrolytic solutions, with the exception that for the ionic cloud Boltzmann statistics are used while for the electronic cloud here under discussion the temperature region is one of complete degeneration.

It is convenient to transform Eq. (65) to one of no dimensions by expressing the distance of the electron from the nucleus in terms of a ground length "a" given by the equation

$$a = (1/Z^{1/3})(3/32\pi^2)^{1/2}(h^2/2me^2), \quad (66)$$

and if the numerical values for h , m and e are inserted we get

$$a = 0.466/Z^{1/3}. \quad (67)$$

Here Z is the atomic number of the element under discussion; we see that the "electronic ground length" varies inversely as the cube root of the atomic number. Correspondingly one can measure the electrostatic potential Φ in terms of a fundamental or ground potential Φ_0 given by $\Phi_0 \equiv Ze/a$ and calling $r/a = \rho$ and $\Phi = \phi\Phi_0$ Poisson's equation becomes

$$\frac{1}{\rho^2} \frac{d}{d\rho} \left(\rho^2 \frac{d\phi}{d\rho} \right) = \phi^{1/2}, \quad (68)$$

where

$$\nu = (Z/4\pi a^3)\phi^{1/2} \quad (69)$$

Eq. (68) was first given by Thomas.³⁷

Now we have seen that the scattering factor for a single electron is given by the expression

$$f^2 = (a_e/R)^2 [(1 + \cos^2 2\theta)/2] F^2(u),$$

whence for an atom having Z planetary electrons we have

$$f^2 = (a_e/R)^2 [(1 + \cos^2 2\theta)/2] Z^2 F^2(u). \quad (70)$$

Now

$$\begin{aligned} Z \cdot F(u) &= Z \int (\sin ksr/ksr) \cdot u \cdot 4\pi r^2 dr \\ &= Z \int (\sin ksr/ksr) (r^2 dr/a^3) \phi^{1/2} \end{aligned}$$

if ν/Z is substituted for u by changing a_H to a .

Now calling $ksr = ksa \cdot r/a = ksa\rho = u\rho$, say we get

$$Z \cdot F(u) = Z \int (\sin u\rho/u\rho) \cdot \phi^{1/2}(\rho) \rho^2 d\rho, \quad (71)$$

where

$$u = ksa = 4\pi a \sin \theta/\lambda,$$

giving

$$F(u) = \int_0^\infty (\sin u\rho/u\rho) \phi^{1/2}(\rho) \rho^2 d\rho. \quad (72)$$

Now the integration has been carried out by Thomas³⁷ and by Fermi³⁸ for the Thomas-Fermi electron distribution. It is shown plotted by Debye³⁹ as $F(u)$ against u , and tables for ρ and ϕ are given by Thomas and in a modified form by Fermi and by Bush and Caldwell,⁴⁰ and for u and F by Bewilogua.⁴¹ The relations between u and F and u and F^2 are shown plotted in Fig. 26. This plot holds for all atoms for which the Thomas-Fermi distribution of electrons is justifiable. To get the atomic scattering factor for any atom, F must be multiplied by the atomic number. Tables of the atomic scattering factors have been given by James and Brindley⁴² for many of the elements, some for the Hartree⁴³ electron distribution, others for the Thomas-Fermi dis-

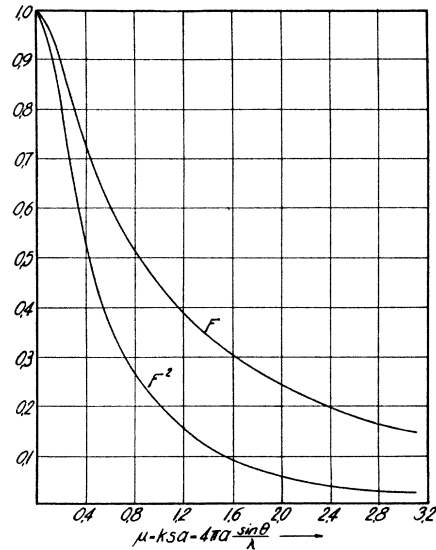


FIG. 26.

tribution. It is known that the Thomas-Fermi distribution holds to a high degree of accuracy for those elements whose atomic number is greater than 23, say, and Bragg and West⁴⁴ have outlined a technique for taking into account the atomic form or scattering factor in the x-ray examination of crystal structures. Since the Debye-Bewilogua curve, (Fig. 26) and the James-Brindley table[†] are both based on the Thomas-Fermi electron distribution there is necessarily exact agreement between the curve and the table.

The curve of Fig. 26 holds for all atoms but the reader should bear in mind that the abscissa involves the "atomic ground length" a and that this is a function of the atomic number, varying inversely as the cube root of the atomic number. Vallarta and Rosen⁴⁵ have lately calculated the influence of relativity upon $F(u)$ for the Thomas-Fermi electron distribution. For practical purposes of crystal analysis it is apparent from their work that the error introduced by ignoring relativity corrections to $F(u)$ are wholly negligible.

7. Form or multiplicity factor

A final factor, called the multiplicity or form factor and variously designated in the literature by n , j , p and z , is equal to unity for the Laue spot and ionization spectrometer (stationary single crystal) methods. For the rotating or oscillating single crystal method and for the powder method its value is equal to the total number of sets of parallel atomic (crystal) planes which contribute to the intensity of a single spot or line due to the fact that, when oriented so as to reflect according to Bragg's law, the reflected rays from each set are directed to the same point and thus superpose. In the rotating (or oscillating) single crystal method this value is dependent upon the orientation and angle of oscillation of the crystal, as well as upon its symmetry, and may be determined only by a study of which ones, and therefore how many, of the sets of parallel planes having "similar" Miller indices (i.e., various sequences of a given $\pm h$, $\pm k$, $\pm l$) will superpose reflections for a given orientation and angle of oscillation of the crystal. For crystals of certain lower order symmetries (parallel face hemihedrism), account

must be taken of whether or not superposed reflections have equal intensities, since for these cases atomic planes having "similar" Miller indices do not always have equal structure factors.

In the powder method (oscillating or stationary) the value of the multiplicity factor depends only upon the symmetry of the crystals. For each of the six divisions of crystal symmetry it is equal to the total number of faces in the holohedral representative of any form (hkl) in question, except that here again for atomic arrangements representing certain types of hemihedrism, hemimorphism, or tetartohedrism different atomic planes (faces) of the given form may have different values of the structure factor. In these cases, if m different values of the structure factor exist, the value of the multiplicity factor equals $1/m$ times its value for the holohedral representative of the form and nS^2 becomes $\sum_p 1^m (n/m)(S_p)^2$. Actually, m can equal only two or four. Otherwise, i.e., if only one structure factor exists for all sequences and changes in sign of a given set of Miller indices, the multiplicity factor is always equal to that for the holohedral form.

Multiplicity factor values may be found in such books as Niggli's *Geometrische Kristallographie des Discontinuums* or Wyckoff's *Structure of Crystals*, First Edition, p. 200, or Second Edition, p. 177.

We have now described the seven factors affecting the intensity of powder photographs, viz., the multiplicity or form factor, n ; the polarization factor, $(1 + \cos^2 2\theta)/2$; the Lorentz factor, $1/\sin^2 \theta \cos \theta$; the atomic structure factor, S ; the atomic form factor, $F(u)$; the Debye temperature factor, e^{-M} and finally the absorption factor, $A(\theta)$. Putting these into a single formula we can say that the relative intensity of the coherent (regular reflection) radiation on a diffraction photograph by the powder method is given by

$$I = n \frac{1 + \cos^2 2\theta}{2} \frac{1}{\sin^2 \theta \cos \theta} |SF_e^{-M}|^2 A(\theta). \quad (73)$$

A word of explanation is needed on the notation $|SF_e^{-M}|^2$. We have seen that instead of Z , in (51) we must substitute Z, F , where F , is obtained from Fig. 26. Several writers have found it

[†] Zeits. f. Krist. 78, 475 (1931).

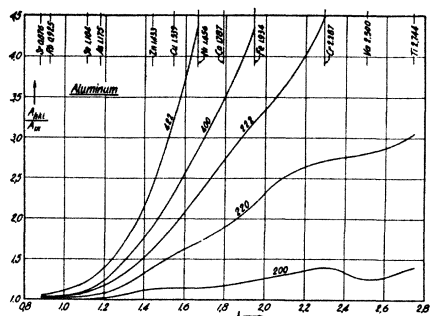


FIG. 27.

desirable to include the e^{-M} in the atomic form factor. It will be shown elsewhere that it is, in general, incorrect to take $S^2|Fe^{-M}|^2$ instead of $|SFe^{-M}|^2$. The error thereby introduced can in certain cases amount to as much as twenty-five percent or more. It must be remembered that S is in general a complex number or revolving vector and that it is only when the several vectors involved in (51) lie along the ± 1 and $\pm i$ axes that $S^2|Fe^{-M}|^2$ would be the same as $|SFe^{-M}|^2$.

If one plots the absorption factor, for certain face-centered crystals as a function of the wavelength, the ordinate in each case being A_{hki}/A_{111} he gets the curves of Figs. 27, 28, 29, r_0 , the radius of the sample tube, being taken in all three figures at 0.2 mm, the customary figure used in Mendenhall Laboratory. These curves were calculated from the curves of Fig. 10 and it is to be expected that the curves of Figs. 27,

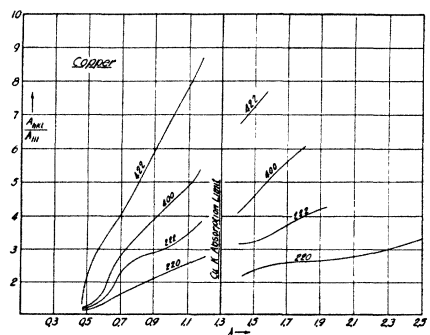


FIG. 28.

28, 29 will have to partake in part of the curvature of some of the several curves of Fig. 10. In Figs. 27, 28, 29 it is assumed that the linear absorption coefficients as a function of the wavelength could be taken directly from Jönsson's tables. Fig. 27 shows at once that for the region of Mo $K\alpha$ -rays the absorption factor can be practically taken as independent of the wavelength. On the other hand for Cu $K\alpha$ -rays the effect of the absorption factor makes it for the 422 face more than three times as strong as it is for the 111 face. Fig. 28 shows that for $\lambda = 0.710\text{A}$ the absorption factor already is strong it becoming for face 422 more than four times as strong as for face 111. The amount of the discontinuity at the K -absorption limit in Fig. 28 is taken from Jönsson. Fig. 29 shows that for Mo $K\alpha$ -rays the

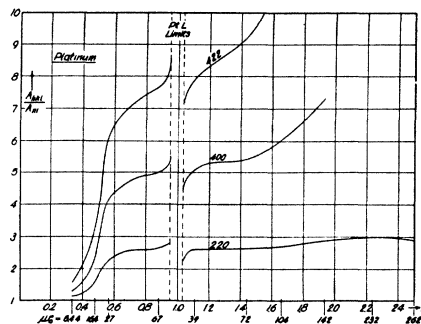


FIG. 29.

absorption factor for face 422 is more than 7 to 1 compared to face 111. The K -absorption limit is to the left of the figure, the L -absorption limits showing at 1.0A. The curves of Figs. 27, 28, 29 stop abruptly a little beyond the last point shown for each curve for the reason that the next point on the curve for a wave-length available in practice would make $2\theta > \pi$ and could not be obtained.

Greenwood²⁵ has put the multiplicity factor, the polarization factor, the Lorentz factor, the temperature factor and the structure factor into an unequivocal column and the atomic form factor and the absorption factor into a doubtful column, that is, a column containing those factors that must be further tested by experiment. It seems to us that it is possible, because of the

work of Professor Debye and his students on the atomic form factor, confirmed entirely by the results of others especially those of W. L. Bragg, R. W. James and other collaborators, to remove, for purposes of x-ray analysis, the atomic form factor from the doubtful column and put it into the unequivocal column.

It is possible to combine the factors in (73) into a smaller number by combining the Thomson and Lorentz factors into a single factor Φ and by combining SF and e^{-M} into a single factor S_0 , say. Then (73) may be written in the form

$$I = n\Phi S_0^2 A. \quad (74)$$

III. COMPARISON WITH EXPERIMENT

Since the powder method is much more of a precision method than any other and since it is the only method available for studying microcrystalline structures like most of the alloys, it becomes of the greatest importance both for science and industry to determine how closely (73) or (74) represents the experimental facts.

IV. CORRECT PROCEDURE IN INTERPRETING THE DENSITOMETER WORK

A few comments on the work of other experimenters are pertinent. Rusterholz is conscious of the correct laws of blackening in the x-ray region for he gives references, e.g., R. Glocker and W. Traub,⁴⁶ where these are elucidated. And yet he apparently makes the mistake of taking the areas under the Moll densitometer peaks as proportional to the intensity. At Mendenhall Laboratory we have compared the Moll densitometer results with those obtained with a photoelectric densitometer, the work of comparison being, of course, taken on the same film and the same part of the film. It was necessary, in order to get the correct answer from both densitometers, to work thus. We plotted the logarithm of the galvanometer readings as we moved by uniform steps across a peak due to the coherent radiation from a given face and then determined the area under the peak on such a plot, the zero line being taken as Rusterholz and others take it, *viz.*, the average line furnished by the background due to coherent and to Compton scattering. For the Moll instrument,

taking the areas direct gave an entirely different answer for a given face from that given by the photoelectric instrument. However, if the logarithm of equidistant ordinates under any peak from the Moll instrument were plotted and the area taken the result by both densitometers is the same. This is clear for the following reasons. (See Eq. (75) below.) Among others, Glocker and Traub⁴⁶ have studied (a) the blackening of a photographic plate due to x-rays as a function of the time for a given wave-length and a given method of developing the plate; (b) the nature of the blackening curve for different wave-length; (c) the determination of the blackening as a function of the product of the ray-intensity and the time (Bunsen's or Schwarzschild's law). The absolute blackening is conveniently defined as the ratio $\log_{10}(I_0/I)$ where I_0 is the intensity of the light beam transmitted by that portion of the developed x-ray film that has not been exposed to x-rays and I is the intensity of the light transmitted by the portion under investigation. It is customary when visual rays are used to divide a blackening curve into three parts, (a) the region of under-exposure where the blackening is almost proportional to the time, (b) that of normal exposure time where the blackening increases with the logarithm of the time and (c) that of over-exposure where the blackening scarcely increases further and finally decreases. Friedrich and Koch⁴⁷ compared visual light and x-rays and obtained the curves of Fig. 30. The light curve has a point of inflection in it near the origin, the part of the curve below the point of inflection corresponding to the under-exposure mentioned, the curve showing the so-called "Schwellenwert." The x-rays on the other hand show none of this wave effect, presumably because in the x-ray region the quantum of energy is so large that any grain of silver salt hit by it is completely reduced to the latent image stage. Friedrich and Koch as well as Glocker and Traub have studied the blackening as a function of the time of exposure. Bouwers⁴⁸ investigated the blackening as a function of the time, for blackenings up to values as high as $2 (= S = \log_{10}(I_0/I))$. In agreement with Friedrich-Koch and Glocker-Traub he found the blackening for small values of S to be approximately linear with time. He agrees with Busé⁴⁹ who found the blackening in

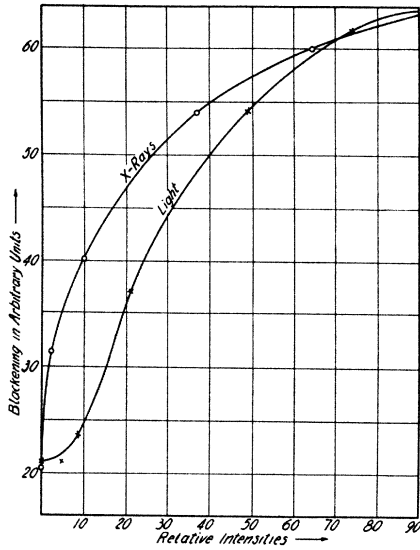


FIG. 30.

the visual region could be represented with considerable accuracy by the formula

$$S = C \log (t/\tau + 1), \tag{75}$$

where C and τ are constants, to be determined empirically. Both Bouwers and Busé found (75) did not hold if a developer were used containing potassium bromide.

Fig. 31 shows Bouwers' results for a plate placed 70, 99, and 140 cm from an x-ray tube taking 2 m.a. x-ray current at a voltage equiva-

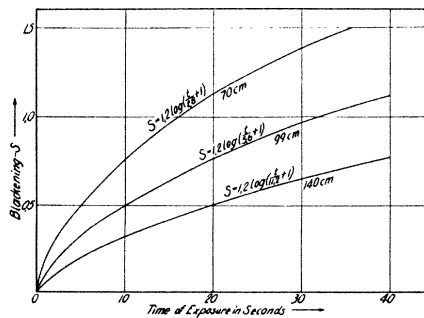


FIG. 31.

lent to 11 cm parallel spark gap, point to plate, the rays being filtered through 2 mm of aluminum. Busé points out that in the work of Toy⁸⁰ the blackening curves taken with visual rays more nearly agree with his work with x-rays the larger the grain size of the photographic emulsion. Busé found the constant C to be a function of the time of development and increases with it according to the formula

$$S_t = S_0(1 - e^{-at}), \tag{76}$$

where a has the value 0.25, nearly.

Bouwers found the blackening as a function of the intensity of the x-rays to be represented by the Schwarzschild⁸¹ relation

$$S = f(I^p), \tag{77}$$

where for ordinary light the exponent p is less than unity but for x-rays it is very nearly unity, his experiments being carried over a range of 9 to 1 for I , giving $p = 0.99 \pm 0.02$. Glocker and Traub found p to be 0.98 ± 0.01 . Taking $p = 1$ one may combine (76) and (77) into the formula

$$S = C \log (It/\tau + 1). \tag{78}$$

Bouwers also investigated the influence of wave-length upon the blackening, finding (78) to hold for the copper, molybdenum and platinum $K\alpha$ -doublets, C being found independent of λ . He found the platinum rays gave a blackening 2.1 times as great as the copper rays.

If in (77) p is accurately 1 in the x-ray region then I and t are equivalent in any exposure and this is the statement of the so called "reciprocity law." Harrison⁸² has shown that the reciprocity law holds in the violet and ultraviolet regions from 4500 to 2500A, he stating that "it cannot be stated definitely whether the small variations of p are real or not," he getting the value 1.06 for $\lambda = 2550A$, for instance. While Jones and Huse⁸³ have shown the failure of the reciprocity law in the visual region, yet, on account of the relatively large value of the quantum of energy in any portion of the x-ray region, the reciprocity law may confidently be expected to hold. The matter deserves further investigation, however, from the violet on down to the shortest x-ray wave-lengths.

Bouwers also investigated the influence of x-ray tube voltage upon the photographic blacken-

ing, keeping the x-ray current constant. The voltage was determined by a parallel point plate spark gap. His results are shown plotted in Fig. 32. He finds the intensity proportional to the square of the applied voltage up to the point where the tube emits the rays characteristic of the anti-cathode, and seemingly above that point to be still proportional to the square of the voltage, the characteristic rays for a tungsten target beginning to be emitted at 67 kv as shown by the change in slope in Fig. 32. Bouwers points out that care should be used in saying that the intensity is proportional to the square of the applied voltage above the threshold value of the characteristic rays because of the jumble between white and characteristic rays and the inability properly to estimate the losses in the tube walls and how this loss depends on wavelength. He also investigated the photographic blackening of continuous x-rays and marked out

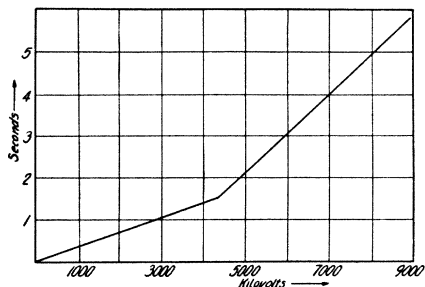


FIG. 32.

a method for getting the distribution of energy in the continuous x-ray spectrum by eliminating the effects of variations of absorption with wavelength. Dorgelo⁶⁴ has summarized as of the year 1925 our knowledge of photographic blackening for both the visual and x-ray regions.

V. TEST OF INTENSITY FORMULA

The intensity formula (73) or (74) is being thoroughly tested in this laboratory. We have stated that the correctness of the polarization factor, the multiplicity factor, the structure factor, the atomic form factor and the temperature factor is generally conceded. The correctness of the Lorentz factor is also generally conceded

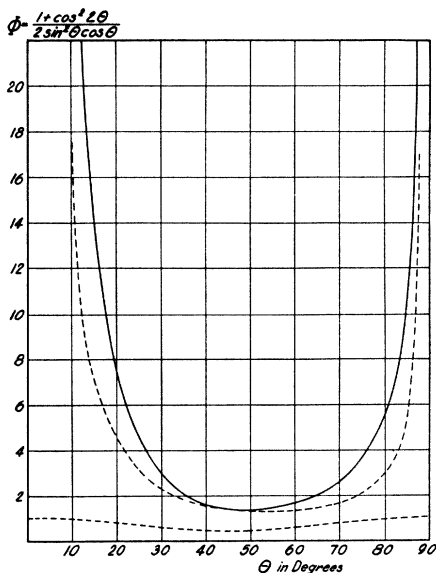


FIG. 33.

but because it rises so abruptly for values of θ larger than 80° , its slope between 80° and 90° being definitely greater than the corresponding complementary angle between 0° and 10° , I have wanted to test its correctness at large angles. Fig. 33 shows the Thomson and Lorentz factors plotted as dotted lines, the full line showing them combined as Φ of Eq. (74).

We have seen how the A factor increases with θ and with λ in such a way that it transcends all other factors for soft x-rays except the Lorentz factor at very large angles. These two factors

TABLE IV. Aluminum powder; λ used 0.710A; $a = 4.0438A$; $\mu r_0 = 0.40$.

Face	n	θ	$\sin \theta/\lambda$	Φ	$A(\theta)$	Fe^{-m}	$I(\text{cal.})$	$I(\text{obs.})$
111	8	8-44-43	0.2142	41.8	48.561	71.6	100	100
200	6	10-6-41	.2473	41.0	48.563	63.4	49.2	50.9
220	12	14-22-33	.3497	14.6	48.599	43.5	32.0	39.0
311	24	16-35-32	.4101	10.4	49.186	33.6	35.5	37.0
222	8	17-42-10	.4283	9.4	49.374	30.6	9.78	9.78
400	6	20-32-21	.4946	6.8	49.950	21.3	3.77	3.73
331	24	22-29-47	.5390	5.5	50.321	16.6	9.46	10.27
420	24	23-6-51	.5530	5.2	50.556	15.3	8.29	10.73
422	24	25-25-11	.6057	4.2	50.985	11.5	5.01	5.05
333	32	27-8-13	.6425	3.63	51.288	9.6	4.84	4.77
511	12	29-46-22	.6994	2.94	51.576	6.6	1.03	—
440	24	31-17-11	.7315	2.63	51.709	5.5	1.53	1.51
600	30	31-46-53	.7419	2.54	51.772	5.0	1.67	—
422	30	31-46-53	.7419	2.54	51.772	5.0	1.67	—

deserve testing for large values of θ , and A for increasing λ . Fig. 27 shows that the influence of A for aluminum powder using molybdenum rays should be very small. Calculation shows it to be only 5 percent greater for face 422 than for face 111. Our preliminary results on aluminum using molybdenum rays are given in Table IV. Two different exposures were made, one of 6 hours, the other of 30 hours, and accordingly for the short exposure face 111 was used as the comparison standard while for the long exposure face 311 was standard since the first three lines of the film had a blackening in excess of 0.6 which is the limit where the blackening as given by (78) is no longer linear. Although the matter is being tested further with more accurate calibration methods, nevertheless the results are sufficiently trustworthy to prove that all of the seven factors except the A factor are correct up to 45° for θ for aluminum, with wave-length 0.710Å. Beyond 45° the general blackening of the film was so great it was impossible to tell whether characteristic lines were present. The A factor is included in the table but the results would be almost as good if it were ignored hence we tried copper rays on aluminum and obtained Table V.

TABLE V. Aluminum powder; λ used 1.539Å; $\mu r_0 = 5.24$.

Face	n	θ	$\sin \theta/\lambda$	Φ	$A(\theta)/A(90^\circ)$	$ F_0-M ^2$	$I(\text{cal.})$	$I(\text{obs.})$	$I(\text{cal.})/I(\text{obs.})$	$A \text{ const.}$
111	8	19-15-0	0.2142	0.786	0.148	71.6	100	100	100	
200	6	22-22-29	.2473	.561	.175	63.4	56.4	56.6	47.7	
220	12	32-34-14	.3407	.241	.289	43.5	54.7	45.7	28.0	
311	24	39-8-34	.4101	.170	.390	33.6	80.3	48.3	30.4	
222	8	41-14-54	.4283	.155	.415	30.6	23.7	23.0	8.5	
400	6	49-43-52	.4946	.136	.537	21.3	14.0	—	3.9	
331	24	56-20-27	.5390	.149	.626	16.6	55.7	17.7	13.2	
420	24	58-20-27	.5530	.158	.659	15.3	37.7	25.9	13.0	
422	24	68-48-59	.6057	.246	.806	11.5	82.3	48.9	15.1	
333 & 511	32	81-29-21	.6426	.662	.948	9.5	286.0	—	44.7	

In this case the agreement is good for the first three lines but it breaks down beyond that, the calculated intensity being too high. Our camera using copper rays was almost a complete circular camera, but it is likely that line 333 (511) did not show up because of baffles which prevented lines having a value of 2θ greater than 160° to show. The camera will be rebuilt so as to get face 333 without question and further tests made. Then we tried Mo-rays on silver powder and got Table VI. It should be stated that for the silver film the calibration was not run at the

TABLE VI. Silver powder; a , 4.077Å; λ used 0.710Å; $\mu r_0 = 6.09$.

Face	n	θ	$\sin \theta/\lambda$	Φ	$A(\theta)/A(90^\circ)$	$ F_0-M ^2$	$I(\text{cal.})$	$I(\text{obs.})$	$I(\text{obs.})/I(\text{cal.})$	$A \text{ const.}$
111	8	8-40	0.212	43.0	0.074	1160	100	100	113	100
200	6	10-2	.245	31.7	.078	1082	54.4	47.9	51.8	51.6
220	12	14-15	.247	15.2	.100	721	44.5	31.1	35.1	32.9
311	24	16-47	.407	10.5	.119	573	58.3	32.2	36.3	36.3
222	8	17-33	.424	9.5	.122	534	18.8	13.3	15.0	10.2
400	6	30-23	.490	6.9	.145	416	8.5	3.6	4.1	4.3
331	24	22-18	.534	5.7	.190	352	26.2	8.4	9.5	12.1
420	24	22-55	.548	5.3	.188	334	24.2	7.2	8.1	10.7
422	24	25-15	.602	4.3	.190	272	18.1	—	—	7.1
333	32	26-54	.637	3.7	.206	236	19.5	—	—	7.0

same time as the intensity work hence the agreement cannot be expected to be very accurate for the first three lines, because for these S was greater than 0.6. Accordingly we chose face 311 as a standard in preference to face 111. A comparison of the last two columns shows much better agreement than that between columns 8 and 10. The result for Mo-rays on silver is the same as for Cu-rays on aluminum—the calculated values are too high.

Work was also done on nickel powder with Mo-rays. The results are shown in Table VII. Again the results are the same—the calculated values are too high.

TABLE VII. Nickel powder; λ used 1.539Å; $\mu r_0 = 21.2$.

Face	n	θ	$A(\theta)/A(90^\circ)$	F^2	e^{-2M}	$I(\text{cal.})$	$I(\text{obs.})$	$I(\text{obs.})/I(\text{cal.})$	$A \text{ const.}$	Wyckoff	$I(\text{obs.})$
111	8	22-18	5.75	0.110	353.4	0.924	100	100	100	100	100
200	6	26-0	4.00	.146	302.8	.897	57.6	43.4	44.5	49.3	49.3
220	12	38-16	1.73	.297	213.2	.810	50.0	18.5	23.2	48.2	48.2
311	24	46-30	1.36	.415	176.9	.748	108.4	28.8	24.8	60.0	60.0
222	8	49-18	1.34	.456	164.4	.729	35.8	8.6	7.4	30.0	30.0
400	6	61-13	1.76	.653	136.9	.657	37.5	6.3	—	—	—
331	24	72-37	3.06	.830	116.6	.607	260.8	34.6	—	126(?)	—
420	24	78-5	4.70	.900	114.5	.590	414.5	49.5	—	—	—

Miss Armstrong⁵⁵ used the ionization chamber method on briquets of copper and iron powders, the wave-length used being the Mo and Cu radiations. The principal object of her experiments was to determine the atomic scattering power of iron and copper. As many others have done she used the intensity formula as a means of determining the atomic form factor and while there is agreement with Debye's F curve for face 111 of copper using Mo-rays, the difference rapidly becomes great with increasing $\sin \theta/\lambda$ such that for face 620 the F value she gets (0.150) is slightly more than half the "correct" value (0.290). Miss Armstrong's values for cop-

TABLE VIII. (Miss Armstrong.) Copper powder; $\lambda 0.710\text{Å}$; ionization chamber method.

Face	π	$\sin \theta/\lambda$	Φ	F^2	e^{-2M}	$I(\text{cal.})$	$I(\text{obs.})$	$I(\text{obs.})$
111	8	0.241	30.85	0.480	0.918	200	222	262
200	6	.278	24.20	.418	.894	100	100	118
220	12	.392	11.60	.286	.800	47.0	60.7	71.7
311	24	.461	8.05	.236	.726	60.8	55.7	65.8
222	8	.481	7.43	.219	.711	17.1	16.1	19.0
400	6	.556	5.16	.180	.640	6.6	5.7	6.7
331	24	.607	4.11	.165	.586	17.6	14.9	17.6
420	24	.620	3.98	.157	.566	15.6	11.2	13.2
422	24	.681	3.15	.135	.520	9.8	7.1	8.4
511 333	32	.723	2.66	.121	.470	8.9	7.6	9.0

per and iron are given in Table VIII. Since she did not consider the A -factor, I have determined the calculated intensity with A -const. from (73) or (74) and show it alongside of her experimental results, face 200 being used as standard. I have also added a second column where face 331 is used as a standard. It is apparent from Table VIII that the A factor when a briquet of powder is used either does not enter into the intensity formula or it enters in the opposite direction from what it does for a cylindrical powder sample. This would be in agreement with expectation on powder briquets using a focussing camera for in a conversation with the writer last August Professor Debye thought absorption could fairly be expected to be independent of θ when the powder exceeded a certain thickness.* This matter is now under test in Mendenhall laboratory.

VI. ANOMALOUS DISPERSION AS REVEALED IN THE DETERMINATION OF THE ATOMIC SCATTERING POWER

Wyckoff⁵⁶ has reported the continuation of Miss Armstrong's work, which was done in his laboratory, and his results are shown for nickel in Table IX along with our own, both taken with Cu-rays. An attempt was made to use the results of Mazza and Nasini,⁵⁷ but their observed results

* The argument for this is that provided the thickness is great enough, when a briquet is used the volume of material irradiated may be said to be the same no matter what the value of θ is, for when θ is small, with a given width of primary beam the penetration is greater than for large values of θ , but the surface area of material irradiated is greater for θ large than for θ small, thus compensating for the lesser penetration, the third dimension of the volume irradiated being independent of θ .

TABLE IX. Nickel; λ used 1.539Å ; $\mu r_0 = 21.2$.

Face	π	θ	Φ	$A(\theta)/A(90^\circ)$	P^2	e^{-2M}	$I(\text{cal.})$	$I(\text{cal.})$	$I(\text{obs.})$
111	8	22-18	5.75	0.110	353.4	0.924	100	100	100
200	6	26-0	4.00	.146	302.8	.897	57.6	43.4	44.5
220	12	38-16	1.73	.297	213.2	.810	50.0	18.5	23.2
311	24	46-30	1.36	.415	176.9	.748	108.4	28.8	24.8
222	8	49-18	1.34	.466	166.4	.729	35.8	8.6	7.4
400	6	61-13	1.76	.653	136.9	.657	37.5	6.3	—
331	24	72-37	3.06	.830	116.6	.607	260.8	34.6	—
420	24	78-5	4.70	.900	114.5	.590	414.5	49.5	—

are expressed qualitatively only and for comparison they used a formula that is now obsolete. Wyckoff used the ionization chamber method, getting reflections from powdered briquets. Since there is good agreement between columns 9 and 10 of Table IX it would appear that one can say that this would seem to verify the statement of Professor Debye that the A factor does not enter into the intensity formula when large blocks of powder are used as samples. On the other hand, there appears to be, by visual inspection of Fig. 1 of Plate IV, Mazza and Nasini, fair agreement between column 8 of Table IX and their results for pure electrolytic nickel, for it would appear that both faces 331 and 420 give reflections stronger than face 111. This is certainly not true, however, of their Fig. 4, taken with "pure commercial" nickel wire, the cold drawing evidently militating strongly as to intensity against the faces having large glancing angles.

Wyckoff worked with copper, nickel and iron using Mo-, Cu-, Ni-, Fe-rays and concludes that the atomic scattering power of an atom varies with wave-length being a minimum near the K -absorption limit of the element and attaining a "maximum at or near its 'resonance' wave-length." What the value of the "resonance" wave-length for nickel is, is not stated. We have run pure nickel with Cu-rays and have inserted our values also in Table IX as the last column. It is seen that they are definitely higher than Wyckoff's values or than the calculated values with A constant, but lower than the values obtained by Eq. (74) (column 8). This confirms the point of view taken in this survey (see below) *viz.*, that the A factor must be modified or the zero line for the densitometer work must be modified from the present experimental practice.

That there is further evidence than that offered by Wyckoff for the atomic scattering power being a function of wave-length is shown in the excellent work done by Bradley and Hope⁵⁸ on iron. They used Mo, Cu, Co, Fe, Cr radiations on an iron aluminum alloy with the composition FeAl. Their sample was in the form of a powder rod and they corrected for absorption by Claassen's method. That the A factor is small for Mo-rays is shown by their results, the ratio A_{420}/A_{100} , with θ changing from $6^{\circ}56'$ to $33^{\circ}30'$ being only 1.164. In Fig. 34 are plotted the results of Bradley and Hope for iron and those of Wyckoff for Ni. It is likely that had Wyckoff been able to have had an anticathode with a wave-length 1.3A his curve for nickel would have been more nearly like that of Bradley and Hope for iron, showing a sharp rise away from the nickel absorption edge on the side of shorter wave-lengths.

We have shown that, provided (74) contains all of the factors that enter into the intensity formula, theory and experiment do not agree (see Tables V, VI, VII, IX) and it becomes very important to know upon which factor or factors to lay the blame. In Bradley and Hope's formula the intensity is given as follows

$$I = k \frac{1 + \cos^2 2\theta}{\sin^2 \theta \cos \theta} n A F^2 = k n \Phi A F^2, \quad (79)$$

where $\Phi = 2\Phi$ of (74) and F^2 stands for $|SFe^{-M}|^2$ of (73). They find the differences they get in F for different wave-lengths to be independent of θ . Consequently whether the A factor were more or less would not materially change the character of their curve (Fig. 34) whereby the atomic scattering factor is definitely lowered across an absorption limit.

Solving (79) for F in the notation of this paper we get

$$F = C(I/n\Phi A)^{1/2}(1/Se^{-M}), \quad (80)$$

it being assumed that for a cubic crystal there is no difference between $|SFe^{-M}|^2$ and $S^2 F^2 e^{-2M}$. Thus the meaning of Bradley and Hope's and Wyckoff's reduction of F across the absorption limit is that A has greatly increased and since for large enough values of μr A varies inversely as μ it is to be expected that F will decrease, for μ is known to decrease with increasing wave-length across the absorption limit. When Mo-

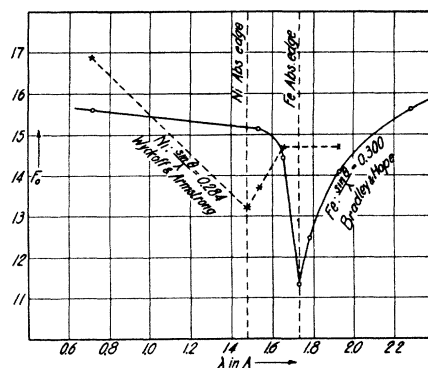


FIG. 34.

rays are used on Mo-powder or Fe-rays on Fe-powder it is always found that the secondary scattering for large values of θ is reduced, more of the energy stays in the coherent rays at the expense of the incoherent rays. The important conclusion of Bradley and Hope that the lowering of F across an absorption limit is independent of θ seems to us to deserve further experimental testing.

It is known from the work of Professor Debye and his collaborators, e.g. Bewilogua,⁴¹ that the ratio of the coherent scattering to the incoherent scattering decreases with increasing θ for atoms and molecules in the gaseous state and since coherent scattering is plainly an atomic property, with the complete lack of knowledge at present as to the relation of the coherent scattering to the physical state of the element under consideration one must first assume complete independence of these two things and this has been done so far in this survey.

Recently Wollan⁵⁹ has surveyed the literature of x-ray scattering and has discussed the atomic form factor. The fact that Wollan⁶⁰ and Harvey⁶¹ have found that the atomic scattering factor for argon and for sylvine, both with atomic number 18, is exactly the same for coherent radiation, in agreement also with James and Brindley's calculations based on Hartree's electron distribution and differing from the Debye-Bewilogua curve (Fig. 26) by ten percent at most for values of $\sin \theta/\lambda$ greater than 0.5, shows that one is probably safe in taking the atomic form factor for

gases and solids the same. Their results indicate, moreover that the Hartree electron distribution is safer to use than the Thomas-Fermi distribution for atoms of low atomic number (see page 43). Jauncey and Harvey⁶² draw attention to the closeness of agreement of the results for argon and sylvine.

The Lorentz factor is being studied in Mendenhall laboratory for large values of 2θ , i.e., for $2\theta > 160^\circ$. Accepting for the moment as unequivocal in (73) the multiplicity, Thomson, Lorentz, structure factor, atomic form factor and temperature† factor the results of Tables V-IX throw doubt on the legitimacy of the A factor as developed by Claassen and Rusterholz and as refined in this survey. All experimenters are agreed that the proper procedure when comparing reflections for different faces is to take the zero as that due to the general blackening or background at the position of the line in question. This procedure must be called in question before the A factor in its present form can be made to assume the blame for the disagreement between theory and experiment for the intensity formula.

In treating the scattering of x-rays from gases, since the earlier literature on this subject mentioned in Compton's *X-Rays and Electrons*, Wentzel,⁶³ Waller,⁶⁴ Compton⁶⁵ and Heisenberg⁶⁶ have all treated this question theoretically, deriving formulas for the total scattering, consisting of the unmodified or coherent scattering and for the modified, incoherent or Compton scattering. In his treatment of the problem Wentzel used quantum mechanics. In his earlier papers Waller used quantum and wave mechanics and later he used Dirac's wave equation together with Dirac's theory of radiation and dispersion. Compton used classical electrodynamics and electron theory, and Heisenberg used wave mechanics.

Calling $(I_0 e^4 / m^2 r^2 c^4)(1 + \cos^2 2\theta) / 2$ the Thomson unit of scattering by an electron in the direction 2θ at a distance r from the electron, e , m and c having their usual significance, Compton showed that the total scattering per atom con-

taining Z electrons is, in our notation

$$I = Z^2 F^2 + Z(1 - F^2) / (1 + \gamma \text{ vers } 2\theta)^2, \quad (81)$$

where $\gamma = h/mc\lambda$. The first term is the coherent scattering and the second the incoherent, its denominator being the Breit⁶⁷-Dirac⁶⁸ factor that comes from the change of wave-length in the Compton effect.

Waller and Hartree⁶⁹ have worked out formulas showing the contributions to the total scattering by the separate electron shells of argon, the necessary summing being done over the wave-functions involved, thus allowing for possible interchange phenomena among the electrons. Herzog⁷⁰ has worked out a method for measuring the scattered x-radiation from gases and has criticized Compton's formula (81) as being too rough an approximation for the incoherent scattering, finding a difference as great as 25 percent between (81) and the Waller-Hartree⁶⁹ formula, which Herzog finds fits his measurements on argon. Wollan⁶⁹ has shown that Barrett's⁷¹ measurements on argon with $\lambda 0.39\text{A}$, his own with $\lambda 0.71\text{A}$ and Herzog's with $\lambda 1.54\text{A}$ fit the same total scattering curve, all in excellent agreement with the Waller-Hartree theory.* Herzog's table I is here repeated as Table X and shows clearly

TABLE X. Argon.

$\sin \theta / \lambda$	$I_{\text{coh.}}$	$I_{\text{incoh.}}$	I_{total}
0	324	0	324
0.065	293.3	1.1	294.4
0.130	223.9	3.5	227.4
0.261	115.8	7.1	122.9
0.391	73.0	9.4	82.4
0.522	54.0	10.8	65.1
0.653	41.9	11.9	53.8
0.783	32.0	12.9	44.9
1.044	16.4	14.4	30.8
1.566	4.6	16.1	20.7
2.088	2.1	16.8	18.9
2.610	1.4	17.2	18.7

that for small values of $\sin \theta / \lambda$ the scattering is all coherent while for very large values it is incoherent. In the region between it is both. Herzog determined experimentally the total scattering from argon and found it was a minimum for $2\theta = 105^\circ$ and rose again for larger values, his last determination being for $2\theta = 160^\circ$. It is inter-

† A recent paper by Jauncey and Pennell (Phys. Rev. 43, 505 (1933)) would put the temperature factor in the equivocal column.

* Wollan, Rev. Mod. Phys. 4, 238 (1932), Fig. 18.

esting that Herzog's measurements on argon give a total scattering curve that is practically identical with that of Scherrer and Staeger⁷² on mercury vapor. There is considerable evidence that the total scattering increases for values of 2θ greater than 160° and it is possible, in crystals at least, that the coherent scattering decreases according to Fig. 26, reaches a minimum and increases again as θ nears 90° . The incoherent scattering theoretically reaches a saturation value for large values of $\sin \theta/\lambda$. Yet many powder photographs that are almost complete circles seem to indicate a definite rise in total scattering as 2θ nears 180° . Examples of this might be said to be Mazza and Nazini's Figs. 1 and 2, Westgren and Phragmen's Fig. 1.* In the work of the latter the length of the film was often 15 cm with a diameter of 5.5 cm giving a half-range, 2θ , of 156° . It will be worth while for work to be done on total scattering both of gases and crystals for values of 2θ beyond 160° .

The question naturally arises, what has the diffuse scattering of gases and crystals to do with formula (73) or (74)? The Bragg law reflection lines of a powder photograph are superposed on the diffuse scattering background, both coherent and incoherent. Because the coherent scattering predominates over the incoherent scattering for small values of θ this fact militates decidedly against the reflection intensities from faces having small Miller indices as compared with those having large indices. The result is that in Tables V, VI, VII, IX, for instance, all the observed values of I for the first few lines are recorded too low compared to those having higher values of θ , thus accounting for the discrepancy between theory and experiment mentioned above. But how to correct for this? Our conclusion is that the zero line of each densitometer peak is below the general background zero and a different amount for every peak depending upon its value of θ and upon the value of λ used. It is well known that the incoherent scattering practically disappears when atoms of large atomic number are used as scatterers. On the other hand, when low atomic number atoms are used the incoherent

scattering is very bad, especially if the wavelength used is shortened or the voltage on the x-ray tube is raised. One must search by cut and try methods to find the proper zero line for each densitometer peak. A good place to begin is to assume even for crystals that the incoherent scattering when corrected by the Breit-Dirac relation is constant for large values of $\sin \theta/\lambda$ and then try in some way to get relative values of the regular reflection intensity compared to the coherent scattering for different θ 's and λ 's. Making theory and experiment agree at some place on the curve, just as Wollan brought a 4 to 2 to 1 change in λ into agreement with one another and with theory in his Fig. 18,† one could assume the A factor correct and find experimentally the corrections needed for different θ 's and λ 's. There would have to be a consistent scheme of correction factors result or else one would have to conclude that the A factor or some other factor needed modification.

A series of papers by Jauncey⁷³ and his collaborators has appeared upon the total diffuse scattering of x-rays by crystals. Certainly it is not known at present how the total scattering changes relatively between the coherent and incoherent parts and also as to their sum as the state of the crystal, e.g., single crystal, crystal mosaic, crystal powder, is changed. In one of his later papers Jauncey⁷⁴ has worked out a method for comparing for gases and crystals the "mass spatial scattering coefficient per unit solid angle" in a given direction 2θ away from the primary beam. Woo⁷⁵ has also been studying the diffuse scattering from gases as well as from crystals and it now appears that Jauncey and Woo have reached common ground in their viewpoints.

Bewilogua⁷⁶ has taken Heisenberg's formula for the incoherent scattering from a gas and reduced it to a form involving for incoherent scattering a fundamental, characteristic or ground-length b similar to the ground-length a that Debye made use of for the coherent scattering. In Bewilogua's notation Heisenberg's formula for the incoherent scattering is given by

$$S_i = Z \left[1 - \int_0^{k_0} k^2 dk \left\{ \left(\frac{\phi(k)}{k} \right)^2 - v \right\}^2 \left\{ \left(\frac{\phi(k)}{k} \right)^2 + \frac{1}{2}v \right\} \right], \quad (82)$$

* Westgren and Phragmen, *Zeits. f. Physik* **33**, 777 (1925).

† Wollan, *Rev. Mod. Phys.* **4**, 238 (1932).

where

$$v = ksa / (6\pi Z) = ksb, \text{ say, where } b = 0.175/Z^{\frac{1}{2}}. \quad (83)$$

In (82) $\phi(\xi)$ is the Thomas-Fermi ϕ -function, ξ being equal to $rZ^{\frac{1}{2}}/a$ where r is one-half the vector sum of the two position vectors entering into the wave-function and its conjugate; ξ_0 , the upper limit on the integral, being given by the equation $(\phi(\xi_0)/\xi_0)^{\frac{1}{2}} - v = 0$. In Fig. 35 is plotted the incoherent scattering, $S = S_i/Z$, as a function of v , together with the Waller-Hartree theoretical value. It is seen that there is almost complete agreement between the two theories, the crosses indicating Heisenberg's values as given by Bewilogua and the curve being the Waller-Hartree results. One should remember that Fig. 35 like Fig. 26 holds for all atoms but that the atomic number is involved in the abscissas of the figure.

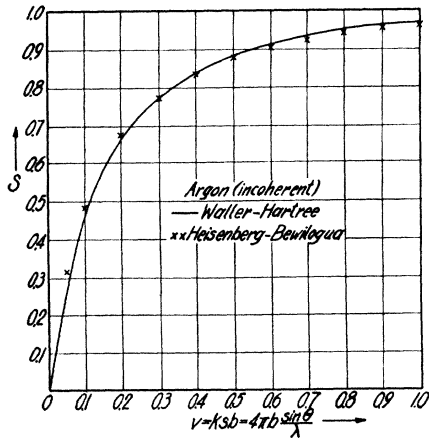


FIG. 35.

One can modify Compton's formula (82) for the total diffuse scattering in accordance with the improvements made by Waller-Hartree and by Heisenberg and thus get

$$I = Z^2 F^2 + ZS / (1 + \gamma \text{vers } 2\theta)^2, \quad (84)$$

where S is the square bracket of (82), i.e., Fig. 35, and F is given by Fig. 26. The writer purposes to plot (84) for all values of $\sin \theta / \lambda$ over the region of wave-lengths customarily available to the x-ray analyst, e.g., 0.2A for tungsten to 8A

for aluminum, say. In carrying this out proper care will be used as to temperature factors involved in F and S . It is hoped in this way to find the correct zero line for the densitometer work in using the intensity formula (73). If success were to attend this effort it would show that the diffuse scattering for gases and crystals is the same. In any case it would be a contribution to the field now being studied by Woo and by Jauncey and his students.†

Attention should be called to the summarizing paper of Ehrenberg and Schäfer⁷⁷ on atomic form factor that has appeared since Wollan's report, and to the recent books like *Ergebnisse der technischen Röntgenkunde, Akad. Verlagsges.*, appearing from the Leipzig school.

VII. CONCLUSION

We have shown in this survey that the formula for relative intensity for the Laue spot method of analysis is

$$I = n \frac{1 + \cos^2 2\theta}{2} \frac{1}{\sin^2 \theta} |S \cdot F \cdot e^{-M}|^2 A(\theta), \quad (85)$$

in which $n = 1$. It is presumed in this formula that white radiation is used as a source.

For the oscillating or rotating crystal method (85) changes to

$$I = n \frac{1 + \cos^2 2\theta}{2} \frac{1}{\sin \theta \cos \theta} |S \cdot F \cdot e^{-M}|^2 A(\theta), \quad (86)$$

provided monochromatic (filtered) rays are used. For this method n is dependent upon the angle of oscillation and upon the crystal symmetry (see page 190). (86) holds also for the ionization chamber method using single crystals. It is known that when working with single crystals careful correction for "extinction" must be made. This is not easy to do. The best practice, e.g.,

† It is possible that a critical study both of (84) and of the recent paper by Jauncey and Pennell, *Phys. Rev.* **43**, 505 (1933) may have to be resorted to, before theory and experiment can be made to agree. The looked-for correction scheme could still be inconsistent if it can be shown that errors due to primary extinction for finely powdered metal crystals are serious. Since these errors would work in the opposite direction from what is found experimentally it would mean that the true zero line is further down than would at first be expected.

reference 33, seems to rest on taking the atomic form factor for atoms at rest on the Hartree distribution (or for high atomic number on the Thomas-Fermi distribution) as standard and correct the measured intensity for each value of θ to this standard. The ionization chamber method can be successfully used in conjunction with the powder method when the powder is in the form of a briquet and the intensity formula becomes

$$I = n \frac{1 + \cos^2 2\theta}{2} \cdot \frac{1}{\sin^2 \theta \cos \theta} \cdot |S \cdot F \cdot e^{-M}|^2, \quad (87)$$

the A factor being taken as constant. This needs further test, however.

For the powder method, provided the powder is sufficiently fine "extinction" errors become negligible and the intensity formula becomes (73). Definite evidence is offered that the usual experimental procedure must be called in question if the Claassen-Rusterholz treatment of the A factor is correct. One can assume the A factor correct and attempt thereby to get an experimental testing of the theoretical formulas for diffuse scattering from crystals both as to the coherent and the incoherent scattering.†

VIII. ACKNOWLEDGMENTS

Grateful appreciation is extended to Messrs. Paul Stanley, A. S. Coffinberry and Jack Ball for help in observations and calculations. My thanks are tendered Mr. Coffinberry and Professor McCaughey for helpful elucidation of the relations between the multiplicity factor and the symmetry of the crystal. I am also indebted to Drs. R. J. Havighurst and P. M. Harris for perusal of the manuscript and for certain suggestions.

BIBLIOGRAPHY

1. M. v. Laue, *Sitz. d. Bayr. Ak. d. Wiss.*, pp. 363-373, M. P. Klasse, 1912.
2. P. Debye and P. Scherrer, *Nachr. Ges. d. Wiss., Goettingen*, 1916; *Phys. Zeits.* 17, 277 (1916).

† The new material of this survey was presented before the American Physical Society at Atlantic City in December, 1932. This is particularly true of Fig. 10, Table II (Fig. 12), Figs. 27, 28, 29, and of most of our results in Tables V, VI, VII and IX.

3. A. W. Hull, *Phys. Rev.* 9, 84 (1916); 10, 661 (1917).
4. W. H. and W. L. Bragg, *Proc. Roy. Soc.* A88, 428 (1913).
5. H. Seemann, *Phys. Zeits.* 20, 169 (1919).
6. E. Schiebold in F. Rinne, *Einführung i.d. Krist. Formenlehre*, 3rd Edition. Pp. 198-200, 1919. See also *Zeits. f. Physik* 9, 180 (1922), and 23, 337 (1924); also *Zeits. f. Krist.* 57, 579 (1923); also F. Rinne, *Formenlehre*, 4th and 5th Edition. Pp. 237-242, 1922.
7. M. Polanyi, *Die Naturwiss.* 9, 337 (1921); *Zeits. f. Physik* 7, 149 (1921).
8. C. G. Darwin, *Phil. Mag.* 27, 315 and 675 (1914); 43, 800 (1922).
9. Bragg, James and Bosanquet, *Phil. Mag.* 41, 309 and 42, 1 (1921).
10. R. J. Havighurst, *Proc. Nat. Ac. Sci.* 12, 375 and 380 (1926); *Phys. Rev.* 28, 869 and 882 (1926). See also *Am. J. Sci.* 10, 15 (1925); *J. Am. Chem. Soc.* 48, 2113 (1926).
- 10a. James and Randall, *Phil. Mag.* 1, 1202 (1926).
- 10b. J. A. Bearden, *Proc. Nat. Ac. Sci.* 14, 539 (1928).
- 10c. E. O. Wollan, *Proc. Nat. Ac. Sci.* 14, 864 (1928).
11. C. G. Barkla, *Phil. Mag.* 15, 288 (1908); Barkla and Ayres, *Phil. Mag.* 21, 270 (1911); E. A. Owen, *Proc. Camb. Phil. Soc.* 16, 161 (1911). See also, R. Pohl, *Die Physik der Röntgenstrahlen* 65, 1912.
12. J. J. Thomson, *Conduction of Electricity through Gases*, 2nd Edition, p. 325.
13. P. Debye, *Ver. d. D. Phys. Ges.* 15, 678, 738 and 857 (1913); *Ann. d. Physik* 43, 49 (1913-14).
14. M. v. Laue, *Ann. d. Physik* 42, 1561 (1913); 81, 877 (1926).
15. C. G. Darwin, *Phil. Mag.* 27, 325 (1914).
16. E. Schrödinger, *Phys. Zeits.* 15, 79 and 497 (1914).
17. H. Faxen, *Ann. d. Physik* 17, 615 (1918); *Zeits. f. Physik* 17, 266 (1923).
18. L. Brillouin, *Ann. de Physique* 17, 88 (1922).
19. I. Waller, *Zeits. f. Physik* 17, 398 (1923); *Dissertation*, Upsala, 1925. See also *Ann. d. Physik* 79, 261 (1926); *Zeits. f. Physik* 51, 213 (1928). See also reference 23.
20. Born and Karman, *Phys. Zeits.* 13, 297 (1912); 14, 15, 65 (1913).
21. M. Born, *Enz. d. math. Wiss.* V3, p. 530 ff.
22. I. Waller, *Dissertation*, Upsala, pp. 4 and 18.
23. Waller and James, *Proc. Roy. Soc.* A117, 214 (1927-8).
24. W. Voigt, *Lehrbuch d. Kristallphysik*, p. 586, Teubner, 1928.
25. T. H. Havelock, *Proc. Roy. Soc.* A105, 488 (1924).
26. R. C. Maclaurin, *Proc. Roy. Soc.* A81, 367 (1908).
27. James and Firth, *Proc. Roy. Soc.* A117, 62 (1927-8).
28. W. Duane, *Proc. Nat. Acad. Sci.* 11, 489 (1925).
29. James and Brindley, *Proc. Roy. Soc.* A121, 155 (1928).
30. A. Rusterholz, *Helv. Phys. Acta* 4, 68 (1931).
31. A. Claassen, *Phil. Mag.* 9, 57 (1930).
32. James, Waller and Hartree, *Proc. Roy. Soc.* A118, 347 (1928).
33. James, Brindley and Wood, *Proc. Roy. Soc.* A125, 401 (1929).
34. C. G. Darwin, *Phil. Mag.* 43, 827 (1922).

35. Debye and Scherrer, *Phys. Zeits.* **19**, 474 (1918); G. Greenwood, *Phil. Mag.* **1**, 963 (1927); Möller and Reis, *Zeits. f. Physik. Chemie* **A139**, 425 (1928).
36. J. A. Bearden, *Phys. Rev.* **29**, 20 (1927).
37. L. H. Thomas, *Proc. Camb. Phil. Soc.* **23**, 542 (1925-7).
38. E. Fermi, *Zeits. f. Physik* **48**, 73 (1928); also *Leipziger Vorträge* p. 95, 1928.
39. P. Debye, *Phys. Zeits.* **31**, 422 (1930).
40. V. Bush and S. H. Caldwell, *Phys. Rev.* **38**, 1898 (1931).
41. L. Bewilogua, *Phys. Zeits.* **32**, 741 (1931).
42. R. W. James and G. W. Brindley, *Zeits. f. Krist.* **78**, 473 (1931); see also *Phil. Mag.* **12**, 81 and 729 (1931). For earlier papers see W. L. Bragg and J. West, *Zeits. f. Krist.* **69**, 118 (1928); G. W. Brindley and R. G. Wood, *Phil. Mag.* **7**, 616 (1929). For still earlier papers see references 8 and 9, also A. H. Compton, *Phys. Rev.* **9**, 29 (1917); Debye and Scherrer, *Phys. Zeits.* **19**, 474 (1918).
43. D. R. Hartree, *Proc. Camb. Phil. Soc.* **24**, 89, 111, 426 (1927-8); **25**, 310 (1928-9).
44. W. L. Bragg and J. West, *Zeits. f. Krist.* **69**, 118 (1928).
45. M. S. Vallarta and N. Rosen, *Phys. Rev.* **41**, 708 (1932).
46. R. Glocker and W. Traub, *Phys. Zeits.* **22**, 345 (1921).
47. W. Friedrich and P. P. Koch, *Ann. d. Physik* **45**, 399 (1914).
48. A. Bouwers, *Zeits. f. Physik* **14**, 374 (1923); *Physica* **3**, 113 (1923); **5**, 8 (1925).
49. A. J. H. Busè, *Mitt. Ned. Nat. Ver.*, 1922; *Physica* **2**, 84 (1922).
50. F. C. Toy, *Phil. Mag.* **44**, 352 (1922).
51. K. Schwarzschild, *Pub. d. v. Kuffnerschen Sternwarte* 1900, 5; *Astrophys. J.* **11**, 89 (1900).
52. G. R. Harrison, *J. O. S. A.* **11**, 341 (1925).
53. L. A. Jones and E. Huse, *J. O. S. A.* **7**, 1079 (1923); **11**, 319 (1925).
54. H. B. Dorgelo, *Phys. Zeits.* **26**, 756 (1925).
55. Alice H. Armstrong, *Phys. Rev.* **34**, 931 (1929).
56. R. W. G. Wyckoff, *Phys. Rev.* **36**, 1116 (1930).
57. L. Mazza and A. G. Nasini, *Phil. Mag.* **7**, 301 (1929).
58. A. J. Bradley and R. A. H. Hope, *Proc. Roy. Soc.* **A136**, 272 (1932).
59. E. O. Wollan, *Rev. Mod. Phys.* **4**, 205 (1932).
60. E. O. Wollan, *Phys. Rev.* **37**, 862 (1931); **38**, 15 (1931).
61. G. G. Harvey, *Phys. Rev.* **38**, 593 (1931).
62. G. E. Jauncey and G. G. Harvey, *Phys. Rev.* **38**, 1071 (1931).
63. G. Wentzel, *Zeits. f. Physik* **43**, 1 and 779 (1927).
64. I. Waller, *Phil. Mag.* **4**, 1228 (1927); *Zeits. f. Physik* **51**, 213 (1928); *Zeits. f. Physik* **58**, 75 (1929). See also James, Waller and Hartree, *Proc. Roy. Soc.* **A118**, 334 (1928).
65. A. H. Compton, *Phys. Rev.* **35**, 1925 (1930).
66. W. Heisenberg, *Phys. Zeits.* **32**, 737 (1931).
67. G. Breit, *Phys. Rev.* **27**, 242 (1926).
68. P. A. M. Dirac, *Proc. Roy. Soc.* **A111**, 405 (1926).
69. I. Waller and D. R. Hartree, *Proc. Roy. Soc.* **A124**, 119 (1929).
70. G. Herzog, *Zeits. f. Physik* **69**, 207 (1931). See also *Helv. Phys. Acta* **2**, 169 and 217 (1929).
71. C. S. Barrett, *Phys. Rev.* **32**, 22 (1928).
72. P. Scherrer and A. Staeger, *Helv. Phys. Acta* **1**, 518 (1928).
73. For references see Wollan, *Rev. Mod. Phys.* **4**, 258 (1932).
74. G. E. M. Jauncey, *Phys. Rev.* **42**, 453 (1932); see also *Phys. Rev.* **39**, 561 (1932). Also Jauncey and Harvey, *Phys. Rev.* **40**, 329 (1932).
75. Y. H. Woo, *Phys. Rev.* **38**, 6 (1931); *Phys. Rev.* **39**, 555 (1932).
76. L. Bewilogua, *Phys. Zeits.* **32**, 740 (1931).
77. W. Ehrenberg and K. Schäfer, *Phys. Zeits.* **33**, 97 and 575 (1932).